2 mif

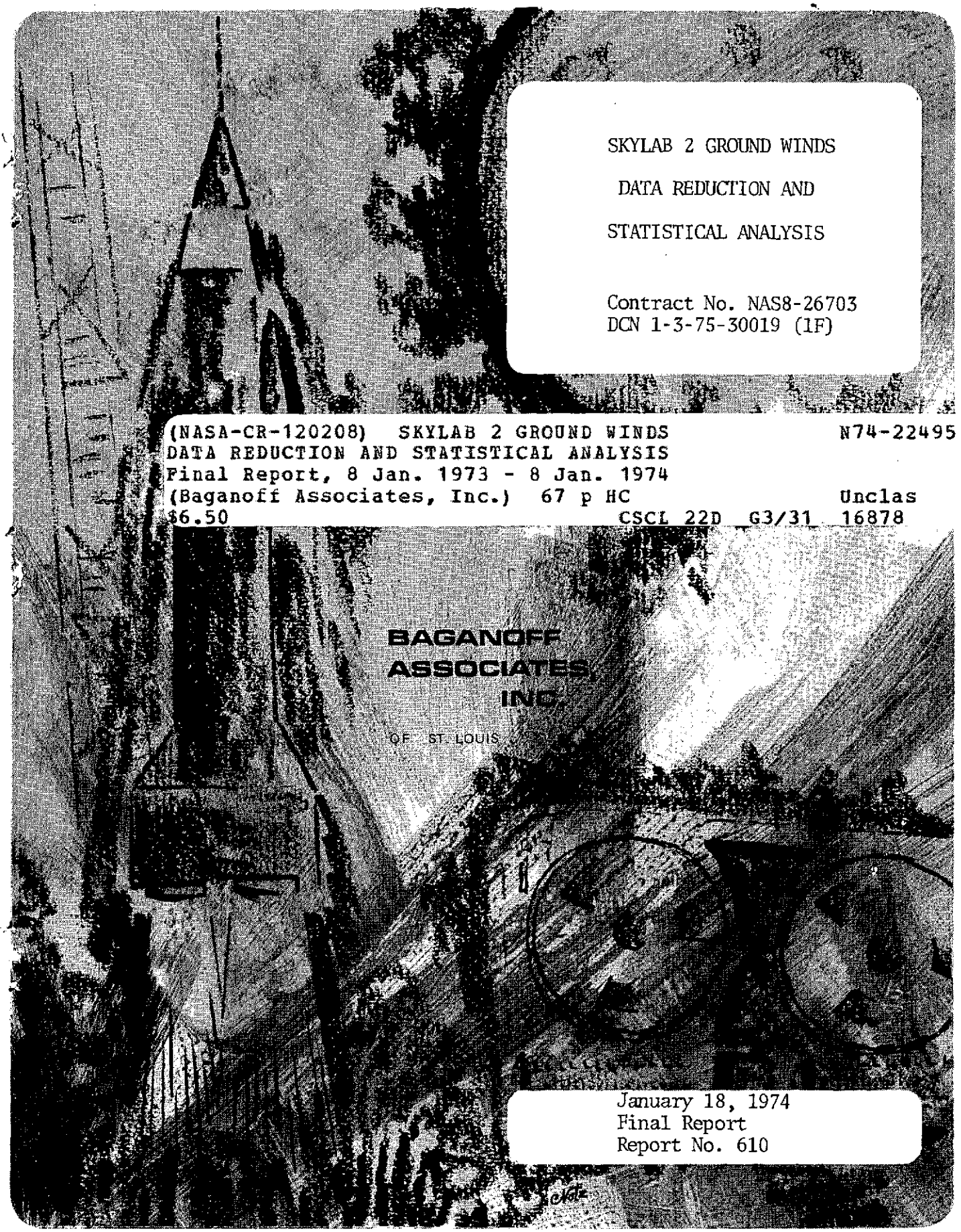

SKYLAB 2 GROUND WINDS DATA REDUCTION AND STATISTICAL ANALYSIS

Contract No. NAS8-26703
DCN 1-3-75-30019 (1F)

BAGANOFF ASSOCIATES, INC.
OF ST. LOUIS

January 18, 1974
Final Report
Report No. 610

BAGANOFF ASSOCIATES, INC.

COMPUTER TECHNOLOGY SPECIALIST
Noise Control, Structural Response, Cross-Correlation Analysis

314-383-2432

6809 West Florissant
St. Louis, Missouri 63136

SKYLAB 2 GROUND WINDS DATA REDUCTION AND STATISTICAL ANALYSIS

FINAL REPORT

REPORT NO. 610 COPY NO. 8

January 18, 1974

Prepared for the George C. Marshall Space Flight Center, Huntsville, Alabama, under Contract No. NAS8-26703, DCN 1-3-75-30019 (1F) covering the period of January 8, 1973 through January 8, 1974.

By Frederick Baganoff

I

Report No.: 610

Date: January 18, 1974

ABSTRACT

A Ground Winds Test was conducted by the Marshall Space Flight Center, Unsteady Aerodynamics Laboratory on the IB/LC-39 vehicle in the fall of 1971. BAI provided on-site engineering at the Langley Research Center, Dynamics Wind Tunnel and later final reduction of the tape recorded data. The Ground Winds Data Reduction System (GWDRS), specifically designed for rapid and inexpensive data analysis was utilized to analyze these tapes for full scale, first and second mode bending moment or acceleration plots versus dynamic pressure or wind velocity.

Select portions of the Skylab 2 tape data was analyzed statistically in the form of power spectral densities, autocorrelations, and cross-correlations to introduce a concept of using system response decay as a measure of linear system damping. The Engineering Notes written also discussed applying these techniques to nonlinear systems. Two small test instruments utilizing the latest LSI circuitry, namely Log-Decrement Dampometer and Autocorrelator Dampometer, were designed and constructed for evaluation.

TABLE OF CONTENTS

1.0 INTRODUCTION

The on-site engineering support provided at the Langley Research Center Wind Tunnel during the Saturn IB/LC-39 Ground Wind Tests and subsequent final reduction of the first mode strain gage data using the Ground Winds Data Reduction System were summarized in BAI Annual Report No. 605. This report also documented the Log-Decrement Dampometer designed and utilized during these tests.

Final analysis for second mode full scale loads using the Ground Winds Data Reduction System on tape recorded second level strain gage signals was performed under contract Amendment (DCN 1-2-75-20055). Plots of dynamic lift, drag and static drag bending moments versus wind velocity or dynamic pressure were produced for 112 Data Points encompassing five fueled vehicle configurations. These final results were transmitted to the COR in an original and one copy of BAI Data Report 607-A.

Final analysis for first mode lift, drag, and resultant acceleration versus dynamic pressure utilizing the GWDRS on the tape recorded x and y accelerometer data at Body Station 121 was continued under Contract Amendment (DCN 1-3-75-30019). An original and two copies of BAI Data Report 608, Volumes I through VI were mailed to the COR as the data reduction was completed.

Statistical analysis in the form of narrowband power spectral densities was conducted on a total of 80 Data Points - tape track combinations to further define the first modal frequencies. These results in the form of digital tabulations and plots were mailed to the COR for use in follow-70 wind tunnel tests conducted in the laboratory.

During this contract, BAI performed introductory studies in the use of computer technology for statistical analysis of multi-modal aeroelastic systems. See Engineering Notes listed in Section (3.2). This effort culminated in the design and construction of an Autocorrelator Dampometer for calculating the system damping ratio under random excitation conditions. A computer simulation program was first written to define the instrument's design parameters before construction began by applying the range of damping ratios encountered in typical wind tunnel tests.

With the advent of micro-processors, a continuous design effort is necessary between the aerodynamicist and the computer technologist in order that the former may avail himself of new measuring techniques not generally available. Results on the evaluation of the Autocorrelator Dampometer on Saturn IB/LC-39 Ground Winds Test data are contained in Section (4.0).

2.0 DATA REDUCTION

2.1) Skylab 2, Second Mode Results - The second level strain gage signals were reduced using the Ground Winds Data Reduction System (GWDRS) for full scale dynamic lift and drag bending moments versus wind velocity and static drag bending moments versus dynamic pressure. The following 112 Data Points were plotted and presented in BAI Data Report 607-A:

74 through 82, 95 through 110: Empty Weight (Secondary Scaling).

161 through 167, 181 through 191: Intermediate Weight (Secondary Scaling) RP1 in S1B State, Spacecraft Fueled.

270 through 322: Completely Fueld (Secondary Scaling).

328 through 349: Completely Fueled (Primary Scaling).

390, 402: Empty Weight (Primary Scaling).

A representative plot of full scale Dynamic Lift Bending Moment versus Wind Velocity is shown in Figure (2.1). The GWDRS also produced the full scale Dynamic Drag Bending Moment versus Wind Velocity plot in Figure (2.2) and the full scale Static Drag Bending Moment versus Dynamic Pressure plot in Figure (2.3).

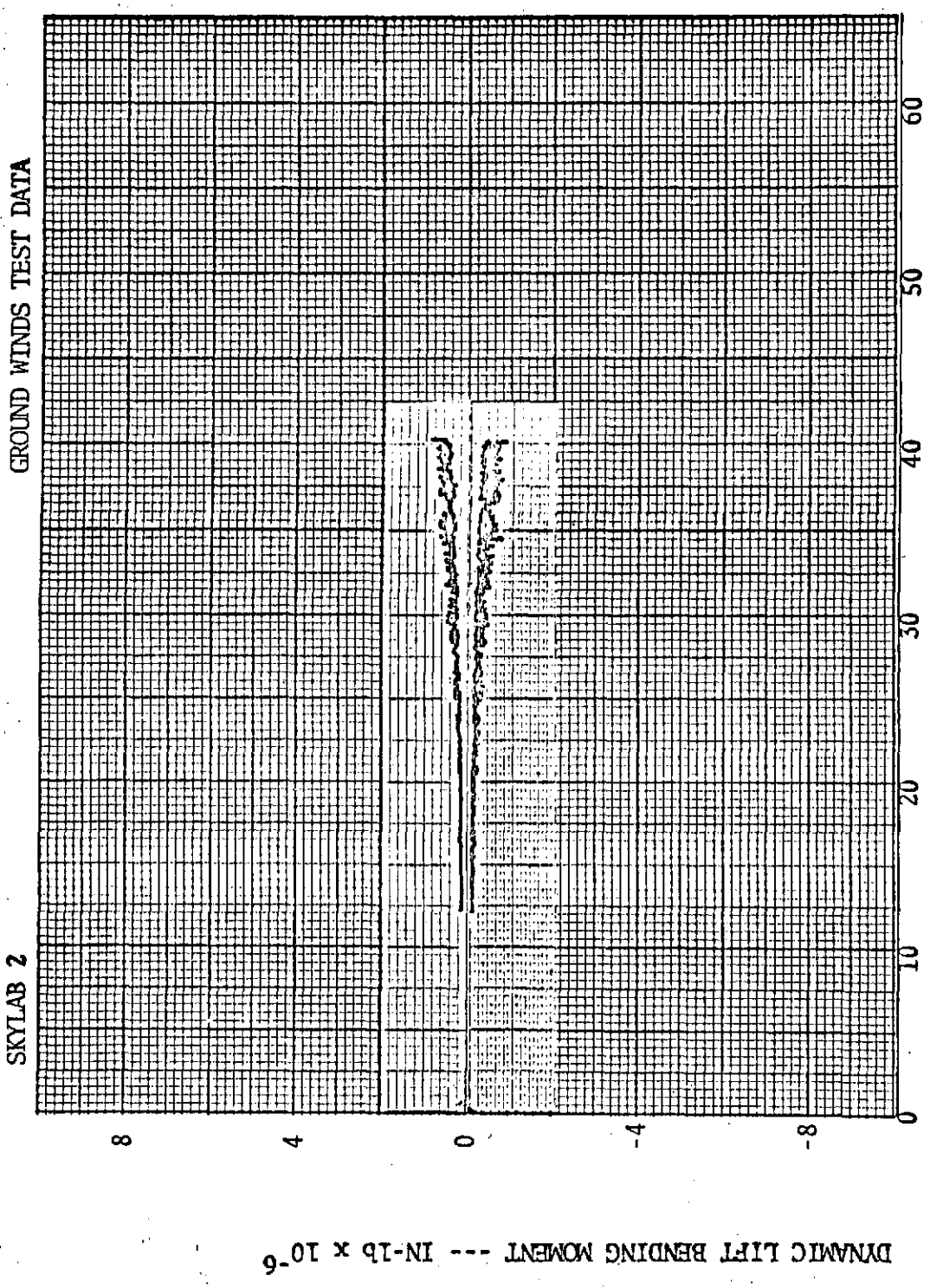
SKYLAB 2
GROUND WINDS TEST DATA
CONFIGURATION: COMPLETELY FUELED (SECONDARY SCALING)
SECOND MODE DYNAMIC LIFT BENDING MOMENT AT STATION 1077.27
WIND TUNNEL AZIMUTH ANGLE 105°
DAMPING 1.0 %, DATA POINT 285
WIND VELOCITY AT STATION 1500 (KNOTS)
0
10
20
30
40
50
60
8
4
0
-4
-8
DYNAMIC LIFT BENDING MOMENT --- IN-lb x 10-6

Figure (2.1)

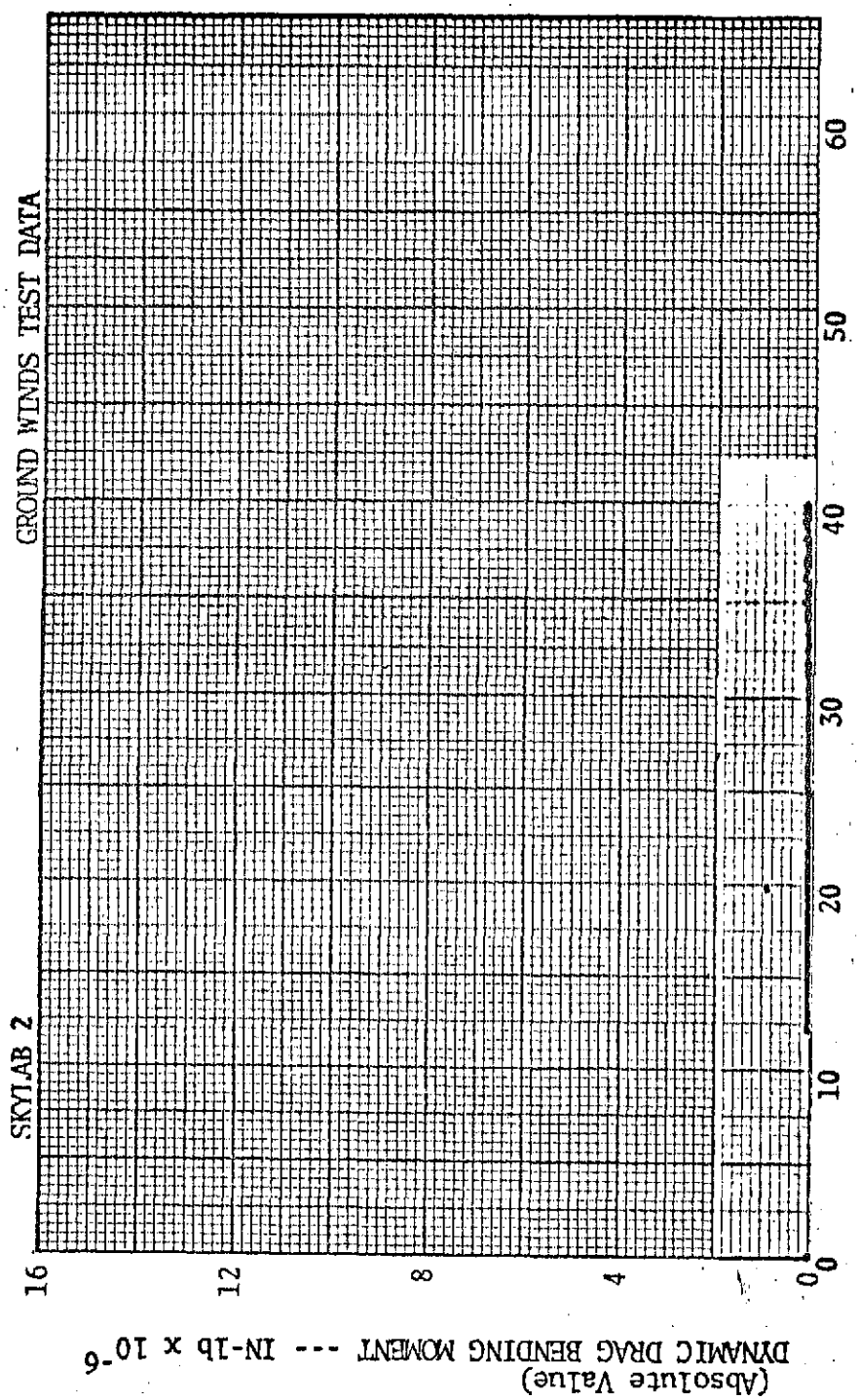
SKYLAB 2
GROUND WINDS TEST DATA
CONFIGURATION: COMPLETELY FUELED (SECONDARY SCALING)
SECOND MODE DYNAMIC DRAG BENDING MOMENT AT STATION 1077.27
WIND TUNNEL AZIMUTH ANGLE 105°
DAMPING 1.0 %, DATA POINT 285
WIND VELOCITY AT STATION 1500 (KNOTS)
0
10
20
30
40
50
60
0
4
8
12
16
DYNAMIC DRAG BENDING MOMENT --- IN-lb x 10⁻⁶
(Absolute Value)

Figure (2.2)

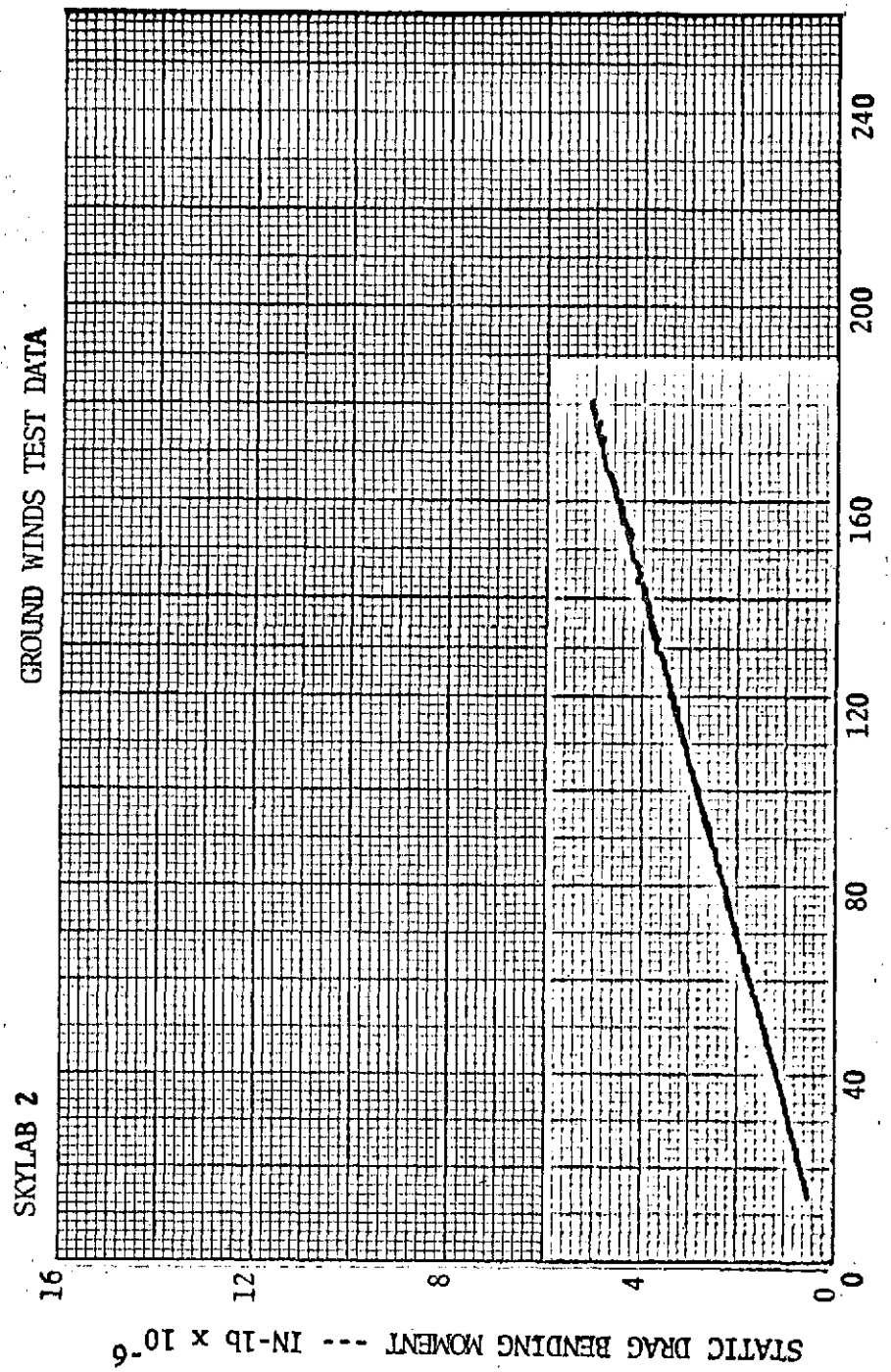
SKYLAB 2
GROUND WINDS TEST DATA
STATIC DRAG BENDING MOMENT --- IN-lb x 10^{-6}
0
4
8
12
16
0
40
80
120
160
200
240
DYNAMIC PRESSURE (PSF)
CONFIGURATION: COMPLETELY FUELED (SECONDARY SCALING)
STATIC DRAG BENDING MOMENT AT STATION 1077.27
WIND TUNNEL AZIMUTH ANGLE 105°
DAMPING 1.0 %, DATA POINT 285

Figure (2.3)

2.2) Skylab 2, First Mode Accelerometer Data - The x and y accelerometer signals derived at Body Station 121 were reduced on the GWDRS to Resultant, Lift and Drag Acceleration versus Dynamic Pressure for Data Points 70 through 157, Empty Weight (Secondary Scaling) Configuration. Representative plots are presented in Figures (2.4), (2.5), and (2.6). These results are contained in BAI Data Report 608, Volumes I through VI.

Report No.: 610

Date: January 18, 1974

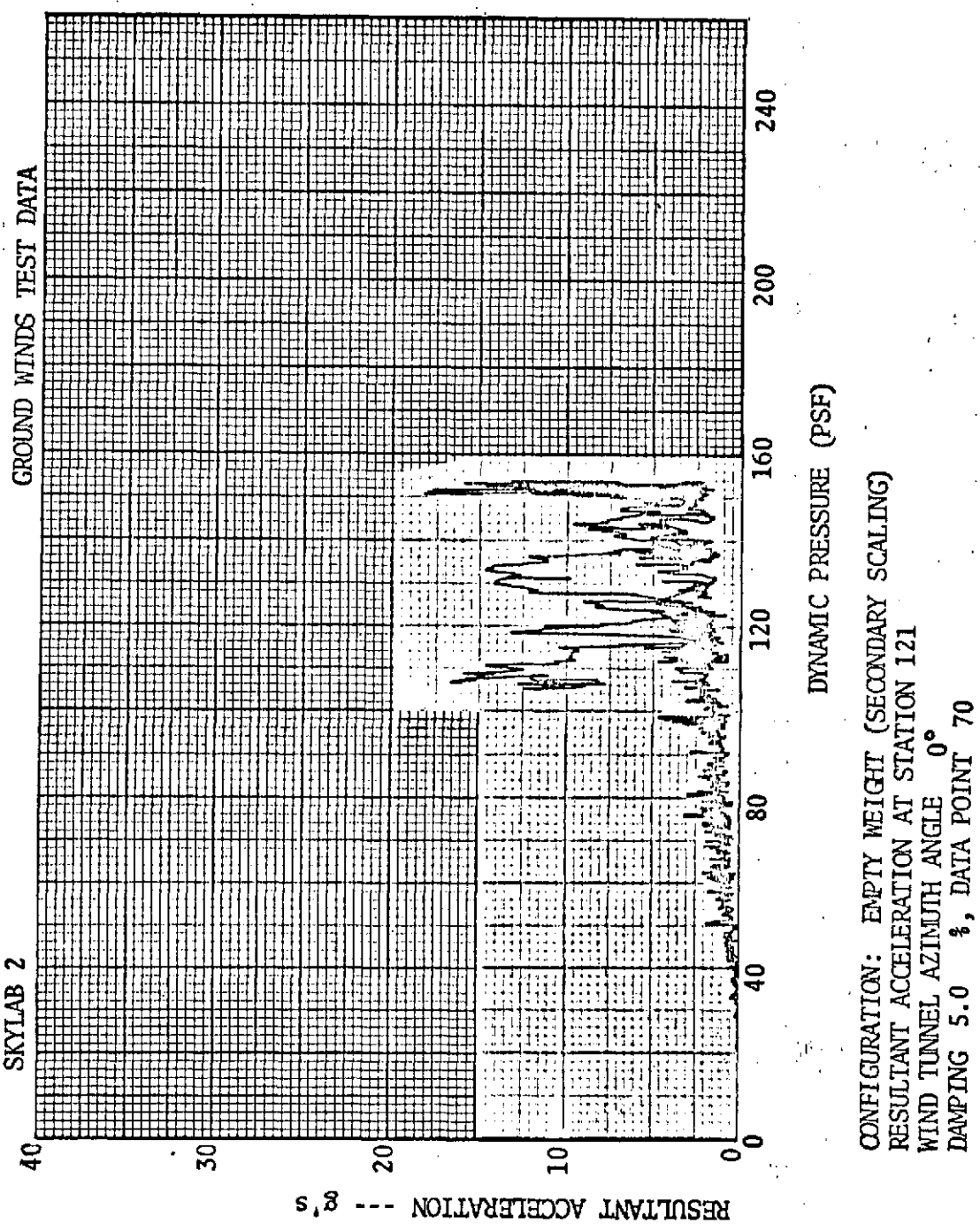

Figure (2.4)

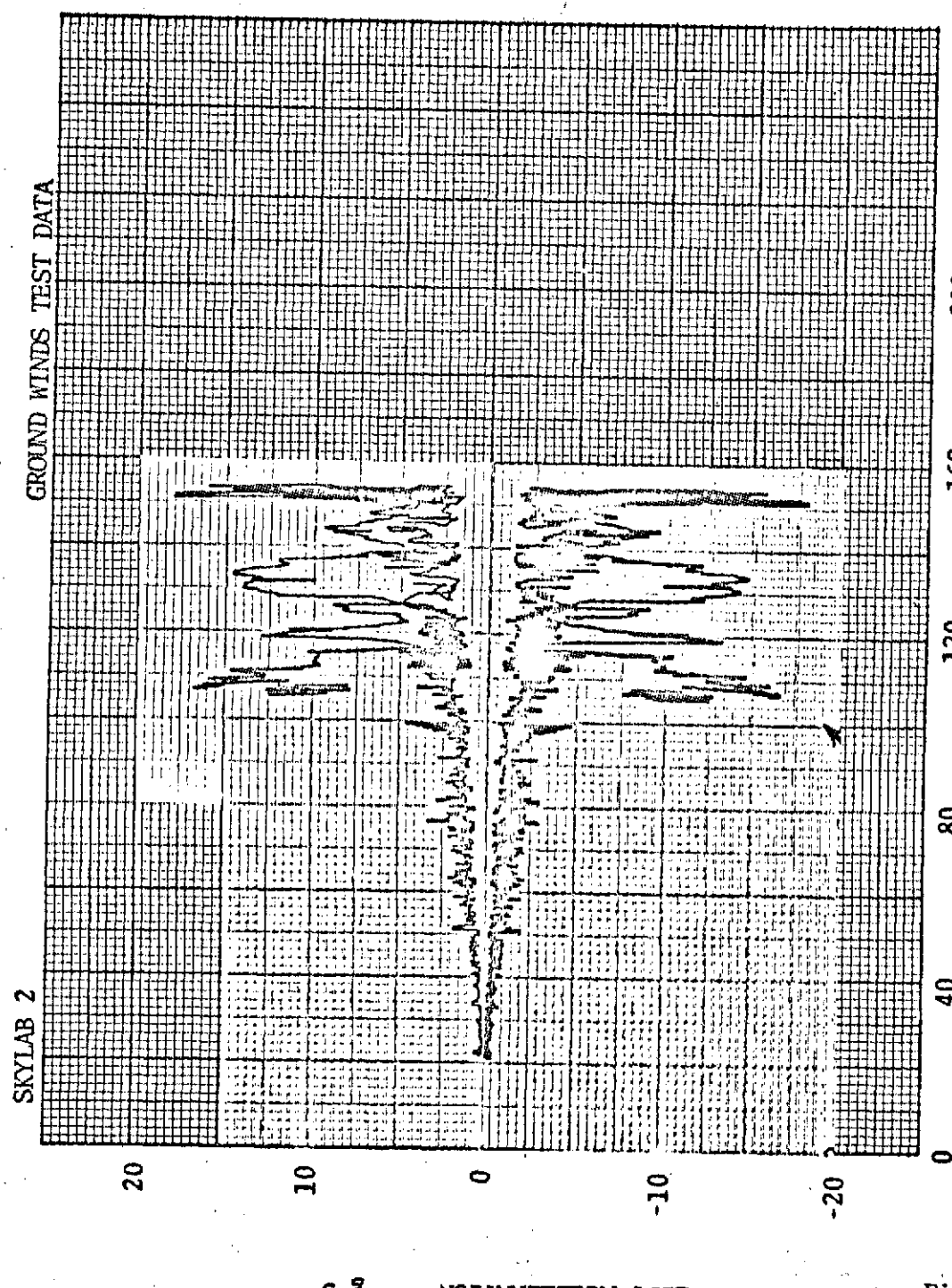
SKYLAB 2
GROUND WINDS TEST DATA
LIFT ACCELERATION --- g's
20
10
0
-10
-20
0
40
80
120
160
200
240
DYNAMIC PRESSURE (PSF)
CONFIGURATION: EMPTY WEIGHT (SECONDARY SCALING)
LIFT ACCELERATION AT STATION 121
WIND TUNNEL AZIMUTH ANGLE 0°
DAMPING 5.0 %, DATA POINT 70

Figure (2.5)

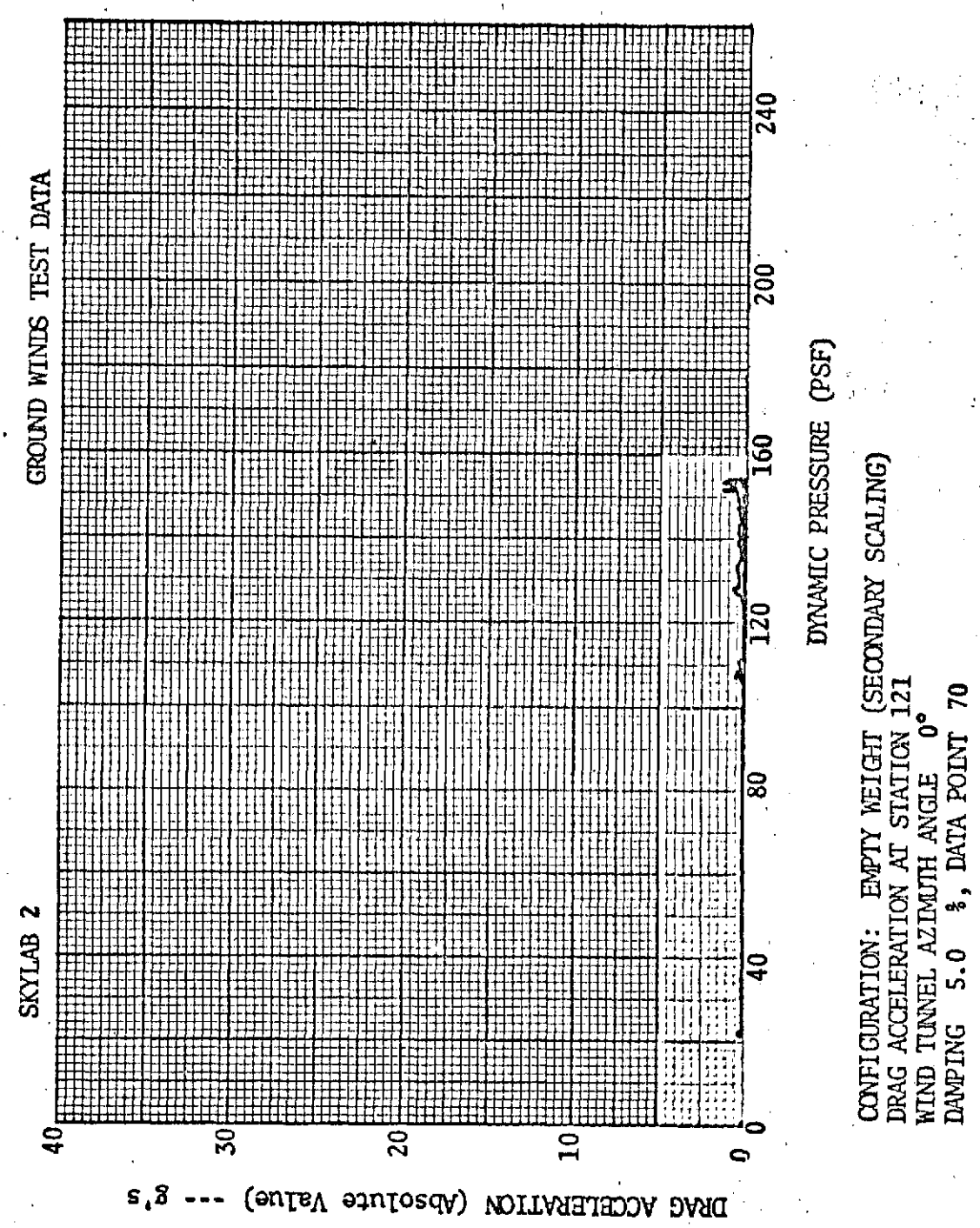
SKYLAB 2
GROUND WINDS TEST DATA
DRAG ACCELERATION (Absolute Value) --- g's
0
10
20
30
40
0
40
80
120
160
200
240
DYNAMIC PRESSURE (PSF)
CONFIGURATION: EMPTY WEIGHT (SECONDARY SCALING)
DRAG ACCELERATION AT STATION 121
WIND TUNNEL AZIMUTH ANGLE 0°
DAMPING 5.0 %, DATA POINT 70

Figure (2.6)

3.0 STATISTICAL ANALYSIS

3.1) Skylab 2, Power Spectral Densities - The Narrowband Analog, Power Spectral Density System was utilized to produce results with a small statistical error. Since a bandwidth of 0.25 Hz was required in order to define the first mode frequencies, an averaging time of 60 seconds was utilized. In all eighty analyses were conducted with a PSD analysis performed at four intervals A, B, C, and D during a sweep Data Point. A typical digital tabulation and corresponding graph are presented in Figures (3.1) and (3.2).

3.2) Skylab 2, Introductory System Damping Studies - Three Engineering Notes were written during this period presenting the results of statistical analysis in terms of autocorrelations and cross-correlations of Skylab 2 data for system damping information. It is firmly believed that statistical techniqes, such as these, will help to formulate an engineering model for predicting an understanding of self-excited system loads.

1) "The Behavior of the Cross-Correlation Function For Viscous Type Damping", January 14, 1972.
2) "Correlation Analysis of Self-Excited Systems", Feb. 28, 1973.
3) "Descriptive Model, Ground Wind Loads," March 27, 1973.

3/6/73

BAGANOFF ASSOCIATES, INC
SKYLAB 2 GROUND WINDS
PSD FIRST MODE

DATA PT.104
TAPE TR. 2
RUN SEC. C
AVE. TIME 60.4 Sec.
B = .25 HZ

	FILTER CTR. FREQ. (HZ)			PSD (V)SQ/HZ	
1	.1500E+02	.1066E+03	.1066E+03	.1581E-05	.1581E-05
2	.1525E+02	.1075E+03	.1101E+03	.1944E-05	.1944E-05
3	.1550E+02	.1080E+03	.1122E+03	.2187E-05	.2187E-05
4	.1575E+02	.1076E+03	.1135E+03	.1974E-05	.1974E-05
5	.1600E+02	.1105E+03	.1152E+03	.3868E-05	.3868E-05
6	.1625E+02	.1105E+03	.1165E+03	.3861E-05	.3861E-05
7	.1650E+02	.1119E+03	.1178E+03	.5408E-05	.5408E-05
8	.1675E+02	.1112E+03	.1187E+03	.4567E-05	.4567E-05
9	.1700E+02	.1127E+03	.1196E+03	.6438E-05	.6438E-05
10	.1725E+02	.1133E+03	.1206E+03	.7424E-05	.7424E-05
11	.1750E+02	.1172E+03	.1222E+03	.1793E-04	.1793E-04
12	.1775E+02	.1172E+03	.1234E+03	.1831E-04	.1831E-04
13	.1800E+02	.1186E+03	.1246E+03	.2515E-04	.2515E-04
14	.1825E+02	.1246E+03	.1276E+03	.9991E-04	.9991E-04
15	.1850E+02	.1281E+03	.1309E+03	.2211E-03	.2211E-03
16	.1875E+02	.1296E+03	.1333E+03	.3175E-03	.3175E-03
17	.1900E+02	.1267E+03	.1342E+03	.1599E-03	.1599E-03
18	.1925E+02	.1231E+03	.1345E+03	.7030E-04	.7030E-04
19	.1950E+02	.1196E+03	.1346E+03	.3165E-04	.3165E-04
20	.1975E+02	.1183E+03	.1347E+03	.2346E-04	.2346E-04
21	.2000E+02	.1181E+03	.1348E+03	.2232E-04	.2232E-04

Figure (3.1)

Report No.: 610

BAGANOFF ASSOCIATES, INC

Date: January 18, 1974

SKYLAB 2 GROUND WINDS

DATA PT. 104 B = 0.25 HZ

CTR. FREQ. INCR. 0.25 HZ

TAPE TRACK 2

AVE. TIME 60.4 SEC

RUN SECTION C

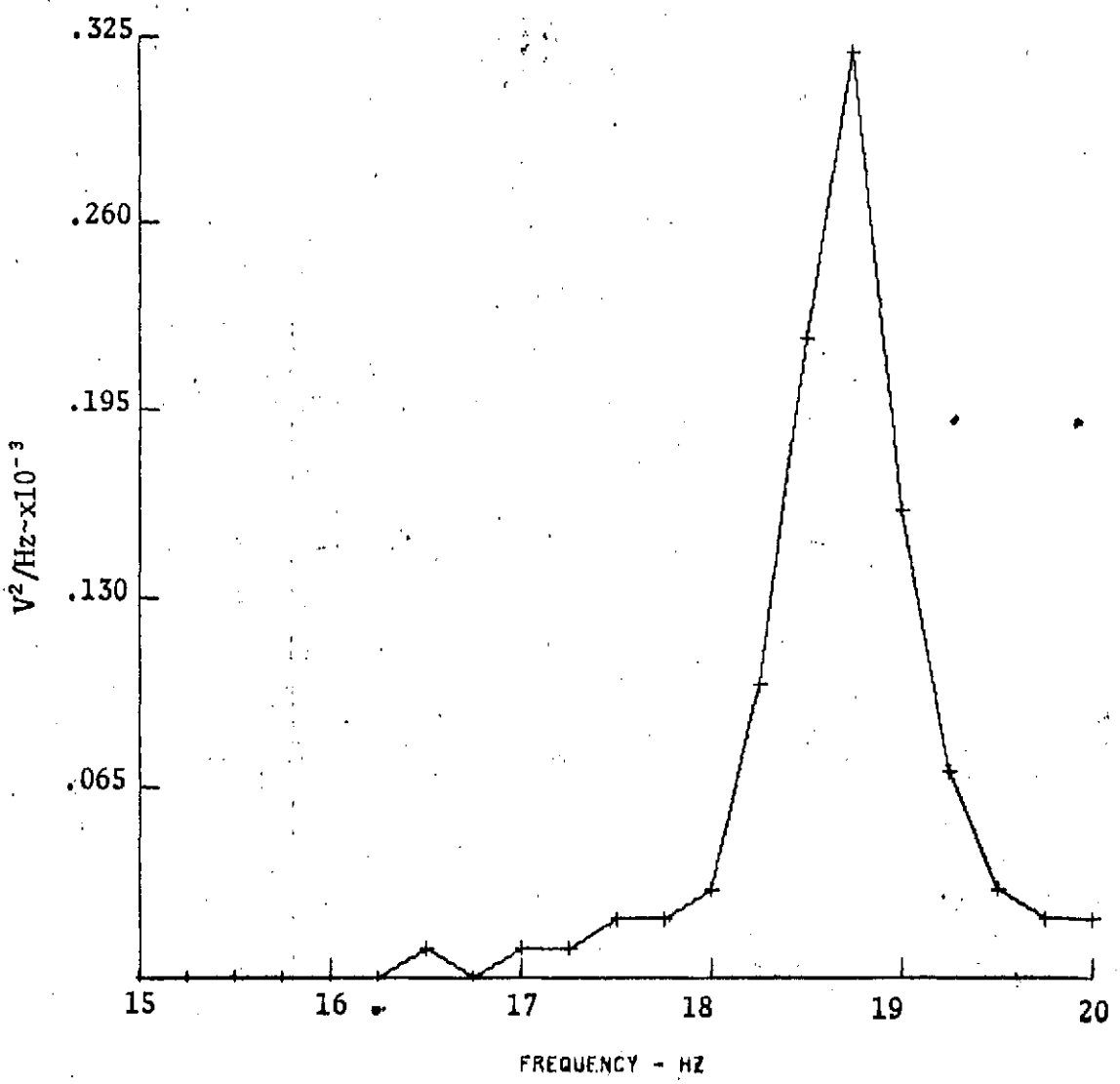

Figure (3.2)

The promising test instrument described in Section (4.0) incorporating ROM's, mini-processors, and RAM's represents a look into the future of wind tunnel testing.

4.0 AUTOCORRELATOR DAMPOMETER

The system damping associated with a wind tunnel model of a launch vehicle subjected to increasing ground winds is an important parameter from the standpoint of monitoring the integrity of the model, and learning about the self-excited flow process. BAI has been in the forefront of developing methodology for using statistical analysis in the form of autocorrelation functions, etc. for the gaining of insight into the closed-loop system composed of the aerodynamic forces and the launch vehicle response. See Engineering Notes listed in Section (3.2). As is the practice in servomechanisms, measurements can be made on the closed-loop system and characteristics of these measurable quantities attributed to the physical parameters of the various elements in the closed-loop, in this case the aerodynamic force and the launch vehicle response.

The Autocorrelator Dampometer described herein was developed under this Contract and represents a small and versatile test instrument that can measure the system damping on-line in the wind tunnel with the wind blowing. This instrument is designed such that when the occasional high peaks in the random response exceed the voltage threshold at the input to the instrument, an input gate enables peak detection circuits to

apply to memory the peak values for the succeeding 32 vibration cycles. These 32 peak values would, in theory, conform to a cosine exponential decay except that the subsequent random inputs to the system cause these peaks to not conform to the free vibration envelope. The electronics in the heart of the instrument multiplies together the peak values and sums these products for succeedingly large delay times tau in the sense of the ordinary autocorrelation function, and the output becomes the systematic impulse response for the system with the effects of the random fluctuation of the input eliminated. This instrument has the advantages that: (1) it operates with peak values which maximize the signal-to-noise ratio and are more easily detected electronically. And (2) the large energy in the peaks is primarily that of the desired vibration mode in a multi-modal system.

An analytical model for a ground winds vehicle falling into the category of self-excited systems is practically non-existent, thus each time a new launch vehicle is designed, a wind tunnel test must be conducted in order to measure experimental loads for various launch configurations and wind velocities and orientations. A predictive model does not exist because empirical data in the form of statistical averages are a rarity since

reliable test instruments for making on-line measurements on a random process are just coming into being.

Off-line, large digital computers are capable of performing the matrix manipulations required in any given statistical analysis once the analog signals have been preconditioned and digitized. Typically, the large computer is required to handle large quantities of data points, and the results are available long after the wind tunnel tests have been completed. The memory capacity of even a disc drive on a mini-computer is soon exceeded if the incoming analog signal is sampled continuously according to the Nyquist criteria. The Autocorrelator Dampometer may be thought of as consisting of two units, first a data compressor to pass only the segments of the data required, and second a matrix manipulator to perform the desired statistical analysis.

The standard procedure in the wind tunnel for obtaining structural damping data is to excite the model sinusoidally with an electromechanical exciter, and then record the free vibration decay on an oscillograph. The desired information is obtained from the log-decrement of the decay envelope. The problems with this method are: (1) expensive wind tunnel time is lost while hand calculations are made, and (2) in multi-modal

systems the decay may pertain to the desired mode for the first few vibrations, and the later smaller vibration cycles pertain to another mode.

Under Contract NAS8-26703, DCN 1-1-75-10052 (1F), an instrument called a Log-Decrement Dampometer was designed and constructed that electronically sampled the peak values of the free vibration signal and computed the log of the ratio of successive peak values, and displayed in decimal notation the average structural damping ratio. This instrument, which occupies approximately 1.3 cubic feet, was utilized in the Ground Wind Tests conducted at LRC on the Saturn IB/LC-39 vehicle in the fall of 1971. This Log-Decrement Dampometer reported in BAI Report No. 605 was found to have its limitation in the wind tunnel environment because, (1) the unit had to be timed with the onset of the free vibration, (2) a multi-modal decay produced an average damping ratio which differed slightly from the desired average, and the supposedly free vibration always contained a random noise background due to compressor motor inputs. The lessons learned using this instrument helped develop added impetus to the already held concept for the Autocorrelator Dampometer. In Figure (4.1) the Log-Decrement Dampometer is the unit shown on top in the picture, and the more recently constructed Autocorrelator Dampometer is

Report No.: 610

Date: January 18, 1974

Figure (4.1)

BAGANOFF ASSOCIATES, INC. Report No.: 610

AUTOCORRELATOR DAMPOMETER EVALUATION Date: January 18, 1974

Dwell Data Point 209 Q = 50 PSF
ϕ = 120° Damping Ratio = .42%

Input: Time History of Base x Strain Gage

Output: Autocorrelation Function Repeated

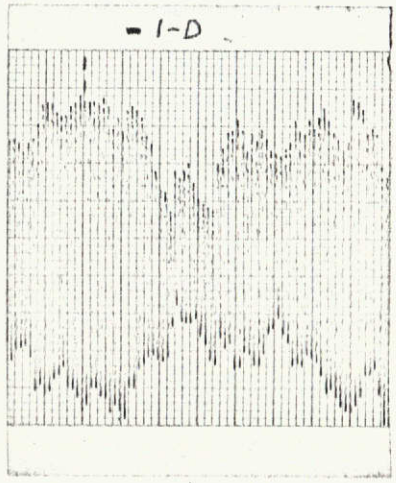

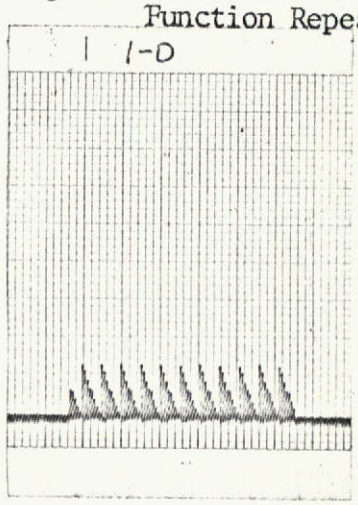

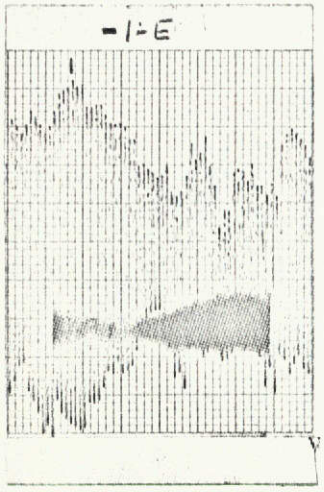

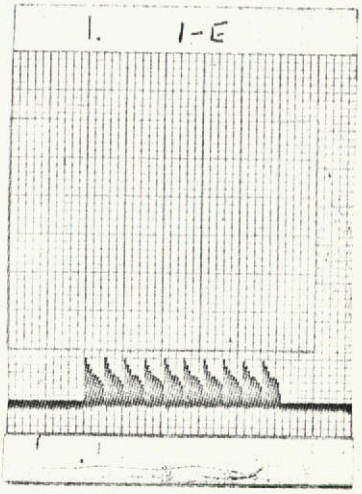

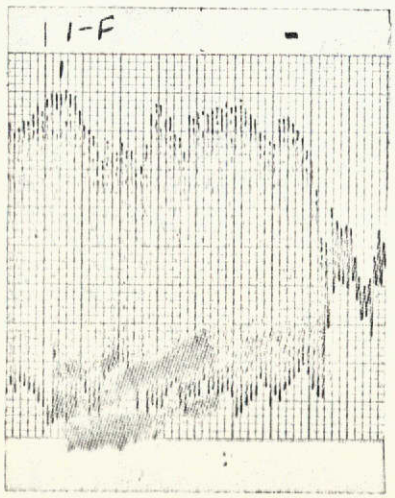

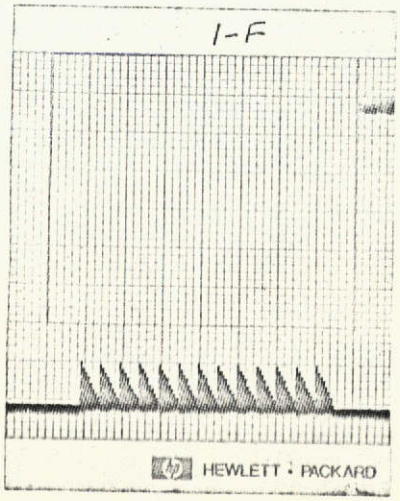

Figure (4.3)

Dwell Data Point 214 Q = 120 PSF
ϕ = 120° Damping Ratio = 1.17%

Input: Time History of Base x Strain Gage

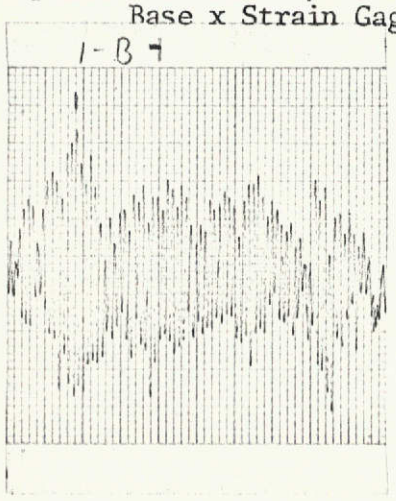

Output: Autocorrelation Function Repeated

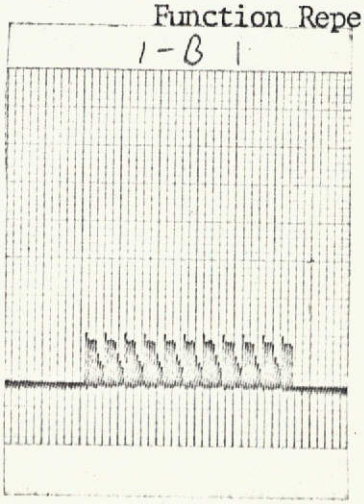

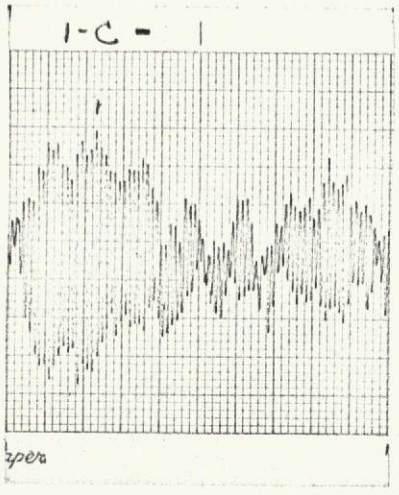

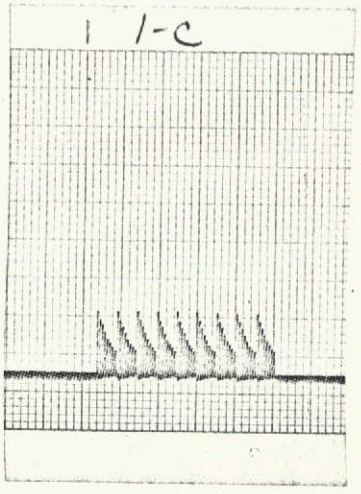

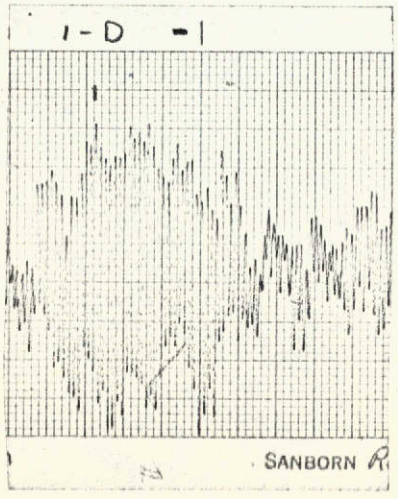

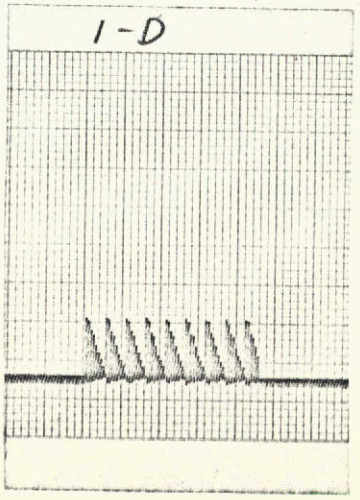

Figure (4.4)

the unit shown on the bottom.

Under the current Contract Amendment, the Autocorrelator Dampometer was designed and constructed which is capable of operating in the wind tunnel while the wind is blowing and thus produce the total system damping ratio. The next section discusses the definition of the autocorrelation function in series form and gives results for a computer simulation encompassing damping ratios from 0.5% to 5% as encountered in the ground wind tests. The simulation showed that the Autocorrelator Dampometer was capable of producing a more ideal linear system, free vibration response as an output even when the input contained two and three slope changes, and also noise modulation. This study determined the optimum number of digital registers required in the unit to be constructed.

4.1) Simulation of the Autocorrelation Function - A computer program was first written to evaluate the effectiveness of the autocorrelation function in determining percent critical damping for the range of values experienced in the Ground Wind Tests. Accurate solutions were obtained for structural damping ratios from 0.5% to 5% and three slope changes during a case single simulated decay.

4.1.1) Autocorrelation Function - The autocorrelation function for stationary signals may be written as:

$$R_{ff(\tau)} = \lim_{T\to\infty} \frac{1}{T} \int_0^T f(t)f(t-\tau)dt \qquad (4.1)$$

Where: R is the autocorrelation function
T is the integrating (averaging) time
f is the waveform of the time function
τ is the delay or time shift

If f(t) is a sampled signal, then Equation (1), (provided N is relatively large) can be approximated by:

$$R_{ff}(kT_s) = \frac{1}{N} \sum_{n=1}^{N} f(nT_s)f(nT_s - kT_s) \qquad (4.2)$$

Where: N is the total number of sample products
k is the total number of sample period shifts
T_s is the sample period

For special application to vibration decay signals, the waveform is an exponentially decaying sinewave. Only the input waveform peaks need to be sampled in order to retain the critical damping information. The output waveform for the autocorrelation function is likewise an exponentially

decaying sinewave and only the peak values are required for extracting the structural damping information. The autocorrelation function in Equation (4.2) can be reduced to a summation of 20 products (first trial) where τ is equal to the period of the input signal.

$$R(\tau_o) = \frac{1}{20} \sum_{n=0}^{19} A_n \circ A_n \qquad (4.3)$$

$$R(\tau_o) = \frac{1}{20} \sum_{n=0}^{19} A_n \circ A_n + 1 \qquad (4.4)$$

$$R(\tau_o) = \frac{1}{20} \sum_{n=0}^{19} A_n \circ A_n + 2 \qquad (4.5)$$

$$R(\tau_o) = \frac{1}{20} \sum_{n=0}^{19} A_n \circ A_n + 3 \qquad (4.6)$$

Where: A_n represents the peak reading of the nth sample.

4.1.2) Test Cases -

An exponentially damped sinewave having a decay rate corresponding to 2% critical damping was selected as the most likely rate to be encountered in wind tunnel tests. Peak readings for 26 cycles of this waveform, serving as input to the computer program, are tabulated in Table (4.2) and plotted in Figure (4.2a). Decay rates corresponding to 0.5% and 5.0% damping were selected as limiting cases to be found in actual tests and peak values for these input waveforms are also found in Table (4.1). To simulate a more realistic waveform as experienced in actual tests, an additional case was generated where the effective damping was allowed to change after eight cycles from 2% to 1% damping as shown on the graph on Figure (4.2b). Still another case was generated by allowing the decay to change again after 12 cycles back to 2% damping.

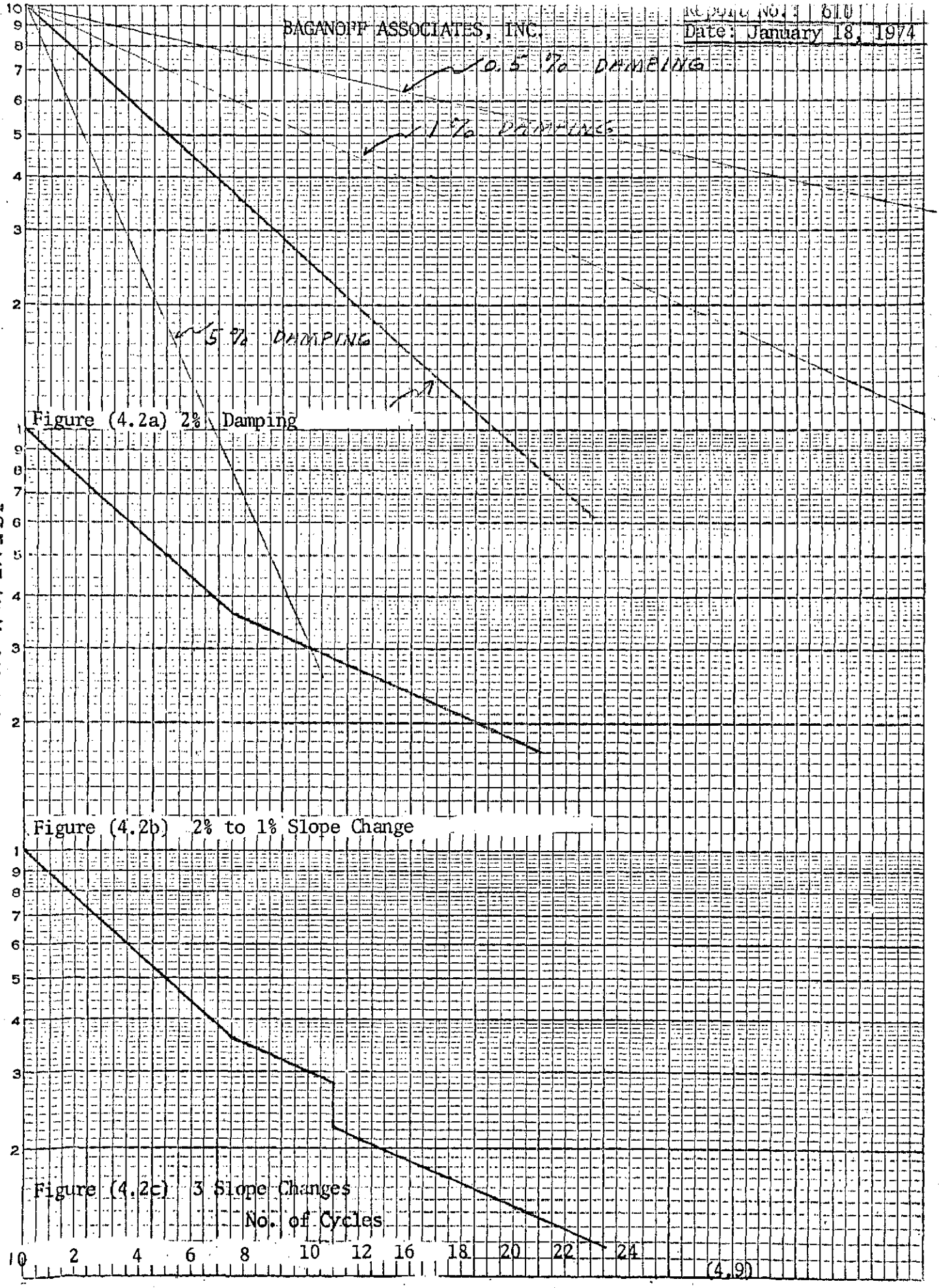

Figure (4.2a) 2% Damping

Figure (4.2b) 2% to 1% Slope Change

Figure (4.2c) 3 Slope Changes

FREDERICK POST COMPANY
311TG370 SEMI-LOGARITHMIC 3 3/4" CYCLES

Peak values for this waveform are tabulated in Table (4.1) and depicted in Figure (4.2c). A third test case was made by applying a 2% modulation to the first decay rate. These values are also tabulated in Table (4.1).

Table (4.1) INPUT PEAK VALUES FOR TEST CASES

Sample No. A_n	0.5% Damping	2% Damping	5% Damping	2% to 1% Damping	3 Slopes	2% Modulation
0	1.000	1.00	1.000	1.00	1.00	1.00
1	.965	.88	.720	.88	.88	.8976
2	.940	.77	.540	.77	.77	.7546
3	.915	.68	.394	.68	.68	.6936
4	.880	.60	.286	.60	.60	.588
5	.855	.53	.210	.53	.53	.541
6	.825	.47	.152	.47	.47	.46
7	.800	.41	.110	.41	.41	.418
8	.770	.365	.079	.365	.365	.37
9	.745	.32	.058	.34	.34	.32
10	.720	.285	.043	.323	.323	.28
11	.700	.25	.031	.305	.305	.25
12	.685	.222		.287	.287	.21
13	.665	.198		.368	.210	.198
14	.645	.174		.25	.197	.174
15	.625	.150		.235	.184	.150
16	.605	.134		.22	.171	.134
17	.587	.118		.205	.160	.118
18	.568	.104		.192	.151	.104
19	.550	.092		.180	.142	.092
20	.532	.081				
21	.515	.071				
22	.500	.063				
23	.487	.055				
24	.470					
25	.458					
26	.443					
27	.428					
28	.415					
29	.402					
30	.390					
31	.377					
32	.364					

4.1.3) Computational Errors For Nominal 0.5%, 2.0% and 5% Damping -

When the various autocorrelation points are computed, the last few

products have zero values because of the time shift of the A_n samples. For example, in computing $R(\tau_1)$ the last multiplication in the summation would be $A_{19} \cdot A_{20}$. Since A_{20} has a zero argument this product will equal zero. An algorithm was derived experimentally that suggested the first sample be used over again for A_{20}, appropriately weighted by a constant, i.e. $A_{20} = k_o A_o$. Therefore, a new set of equations would result for $R(\tau)$ and as shown below:

$$R(\tau_0) = \frac{1}{20} \sum_{n=0}^{19} A_n \circ A_n \tag{4.8}$$

$$R(\tau_1) = \frac{1}{20} \sum_{n=0}^{19} (A_n \circ A_{n+1} + A_{19} \cdot k_o A_o) \tag{4.9}$$

$$R(\tau_2) = \frac{1}{20} \sum_{n=0}^{19} (A_n \circ A_{n+2} + A_{18} \cdot k_o A_o + A_{19} k_1 A_1) \tag{4.10}$$

$$R(\tau_3) = \frac{1}{20} \sum_{n=0}^{19} (A_n \circ A_{n+3} + A_{17} \cdot k_o A_o + A_{18} \cdot k_1 A_1 + A_{11} k_2 A_2) \tag{4.11}$$

$$R(\tau_4) = \frac{1}{20} \sum_{n=0}^{19} (A_n \circ A_{n+4} + A_{16} \cdot k_o A_o + A_{17} \cdot k_1 A_1 + A_{18} \cdot k_2 A_2 + A_{19} \cdot k_3 A_3) \tag{4.12}$$

The values of k_0 through k_3 are calculated from the following equations:

$$K_o = \frac{A_{20}}{A_0} \tag{4.13}$$

$$K_1 = \frac{A_{21}}{A_1} \tag{4.14}$$

$$K_2 = \frac{A_{22}}{A_2} \tag{4.15}$$

$$K_3 = \frac{A_{23}}{A_3} \tag{4.16}$$

Using the input peak values for Test Case 2, $R(\tau_0)$ through $R(\tau_4)$ were

computed using both sets of Equations (4.3) through (4.7), and the Modified Equations (4.8) through (4.12). Values of $R(\tau)$'s are listed in Table (4.2) below:

Table (4.2)

$R(\tau)$ Computations for 2.0% Nominal Damping Data and 20 Memory Locations and Extended Memory

	$R(\tau)$ 20 Locations	$R(\tau)$ Extended Data
τ_0	.2216	.2216
τ_1	.1948	.1952
τ_2	.1712	.1719
τ_3	.1506	.1518
τ_4	.1324	.1340
Computed Damping	(2.00%)	(2.00%)

Both sets of computations: (1) summations containing 20, 19, 18 --- products and (2) summations containing a constant 20 products, produced the same answer for the computed damping of 2.00%. The implementation using 20 fixed locations and no natural extension of the input data gave identically 2.00% damping because the quantities of A_{17} --- A_{20} were small to begin with.

The extended data solution in Table (4.3) gives the almost perfect answer of 0.49%, meaning that 36 memory locations would be the most desirable. Thirty-two memory locations produce the next best result, of 0.64 % damping and the remaining case 1.0%. Tentatively, an autocorrelator incor-

porating 32 memory locations might be the best compromise if the results for 5% critical damping are satisfactory.

Table (4.3)

$R(\tau)$ Computations for 0.5% Nominal Damping Data and 20 and 32 Memory Locations and Extended Memory

	$R(\tau)$ 20 Locations	$R(\tau)$ 32 Locations	$R(\tau)$ 32 Locations, Extended Data
τ_0	.5845	.4426	.4426
τ_1	.5517	.4246	.4289
τ_2	.5196	.4070	.4156
τ_3	.4877	.3898	.4027
τ_4	.4561	.3728	.3900
Computed Damping	(1.0%)	(.64%)	(.49%)

Since for 5.0% damping the A_n's decrease rapidly to small magnitudes, 20 memory locations produced a very satisfactory answer 4.98%, and 32 data locations would not improve it.

Table (4.4)

$R(\tau)$ Computations for 5.0% Nominal Damping Data and 20 Memory Locations

	$R(\tau)$ 20 Locations
τ_0	.1069
τ_1	.0780
τ_2	.0576
τ_3	.0419
τ_4	.0304

4.1.4) Computational Errors for Changes in the Decay Slope -

Peak magnitudes for this evaluation are tabulated under heading 2% to 1% Damping, in Table (4.1). Using the unmodified Equations (4.3) through (4.7), (no extension of the input data) the resulting $R(\tau)$'s are listed in Table (4.5)

Table (4.5)

$R(\tau)$ Computations for Nominal 2% to 1% Damping Slope Change

	$R(\tau)$ 20 Memory Locations
τ_0	.2367
τ_1	.2096
τ_2	.1857
τ_3	.1651
τ_4	.1470
Computed Damping	(1.97%)

The computation of structural damping for the primary mode of interest in a model, 1.97% is reasonably accurate with the contribution from the unwanted mode, 1% damping, practically excluded.

4.1.5) Computational Errors For Decay Slope of 2% to 1% and Back to 2% -

The peak input values for this evaluation are tabulated under the heading "3 Slopes", in Table (4.1). Using Equations (4.3) through (4.7), the following solutions for $R(\tau)$ were computed.

Table (4.6)

$R(\tau)$ Computations for Decay Slope of 2% to 1% and Back to 2%

	$R(\tau)$
	20 Memory Locations
τ_0	.2301
τ_1	.2030
τ_2	.1793
τ_3	.1588
τ_4	.1409
	Computed Damping
	(1.97%)

The computed critical damping of 1.97% is a good approximation to the nominal damping of 2.0% representing the damping of the vibration mode of interest in the structure.

4.1.6) Computational Errors For Input Data Composed of 2% Nominal Damping Plus 2% Noise Modulation -

For this simulation, the values under the heading "2% Damping" in Table (4.1) were alternately increased and decreased by 2%. The resultant input data are entered in the last column of Table (4.1) and the answers for $R(\tau)$ are listed in Table (4.7) following.

Table (4.7)

$R(\tau)$ Computations for 2.0% Nominal Damping
Plus 2% Noise Modulation

	$R(\tau)$ 20 Memory Locations
τ_0	.2227
τ_1	.1958
τ_2	.1713
τ_3	.1515
τ_4	.1326
Computed Damping	(2.02%)

As shown, the autocorrelation process reduced the 2% noise modulation of the input data to 1% modulation of its output. The S/N improvement was probably better than this, but the slope on the semi-log paper could not be read more accurately.

4.1.7) Autocorrelator Design Detected By Structural Damping Accuracies -

From the computer simulated tests, it was demonstrated that the autocorrelation function is an effective means of reducing the noise in a vibration decay signal and at the same time preserving the structural damping information. It is also concluded that 32 data storage cells in the autocorrelator were sufficient to produce acceptable results for input signals corresponding to 0.5% to 5% critical damping.

4.2) Autocorrelator Dampometers Logic Diagrams - As shown in Figure (5.3), the unit contains a trigger level adjustment and Peak Detector at its input. The trigger level adjustment allows the operator to select the magnitude of the incoming strain gage signal at which the Digitizer Control passes on an enabling trigger signal to the Analog-to-Digital Converter. The Peak Detector only presents an output when an incoming signal peak has occurred. The Analog-to-Digital Converter converts the following 32 peak analog voltages to digital words, and stores them in the Random Access Memory (RAM). The Read Only Memory (ROM) represents a mini-programmer for manipulating the words in memory and calculating the autocorrelation function. Complete documentation of the Autocorrelator Dampometer is contained in Figure (5.2) in the form of Logic Diagrams, Circuit Diagrams, and Wiring Diagrams.

4.3) Skylab 2 System Damping Results - Data Points 209 and 214 from the wind tunnel series represented dwell conditions of 50 and 120 PSF respectively. These two runs at an azimuth angle of 120° produced relatively large vehicle responses and these were analyzed previously for damping information by both analog and digital computer techniques. See Engineering Notes. Data Point 209 related to a tunnel velocity giving the critical Strouhal frequency and a system damping ratio of 0.42% while

Data Point 214 gave a system damping ratio of 1.17%.

Figure (4.3) shows a time history of the strain gage signal applied to the Autocorrelator Dampometer and the autocorrelation function at its output for three different segments of Data Point 209. In each case, a pencil mark notes the extreme peak where the Analog-to-Digital Converter first began operation. The 32 subsequent peaks were then digitized. The right-hand time histories show the autocorrelator function repeated on a very time contracted scale. This repeating action is necessary for refreshing the image of the autocorrelation function on an oscilloscope for operator viewing.

The first time history segment (1-D) presented in Figure (4.3) for Data Point 209 depicts 32 successively decreasing peak values beginning with the pencil mark. The Autocorrelator Dampometer output supports these observations of the input by portraying a rapidly decreasing stairstep function corresponding to $\tau = 0$ and the first seven time lags. Time segment (1-E) depicts rapidly decreasing peak values for a time, and then the peak values remain at constant amplitude. The Autocorrelation output in (1E) can be seen to duplicate these findings. In time segment (1-F), it can be seen that the peak values decrease for a time, and then begin to increase before 32 peaks have been accounted for. The autocorrelation out-

BAGANOFF ASSOCIATES, INC. Report No.: 610

AUTOCORRELATOR DAMPOMETER EVALUATION Date: January 18, 1974

Dwell Data Point 209 Q = 50 PSF
ϕ = 120° Damping Ratio = .42%

Input: Time History of Base x Strain Gage

Output: Autocorrelation Function Repeated

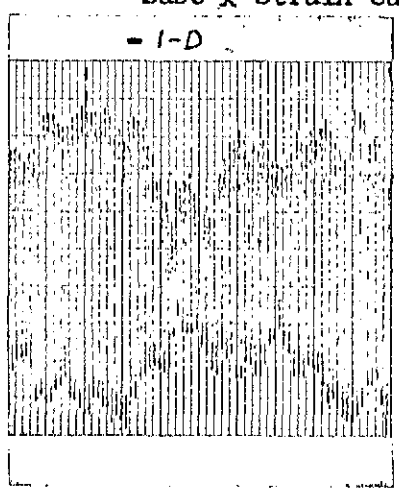

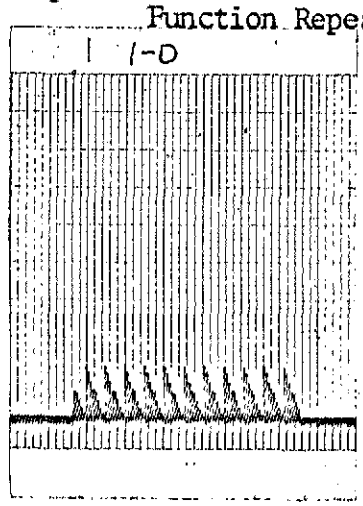

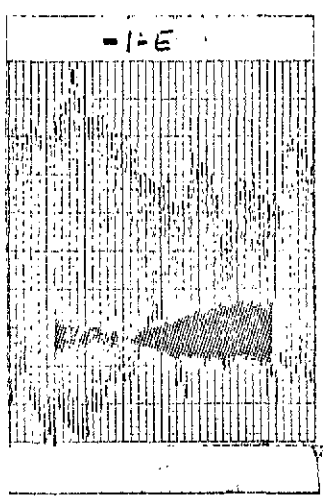

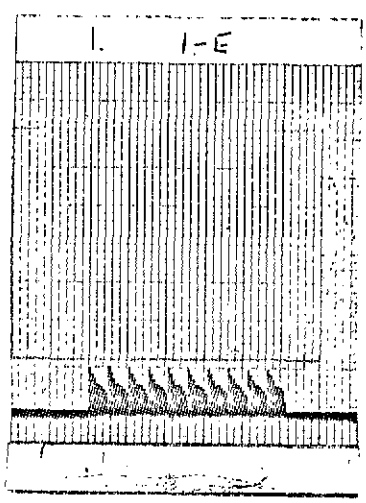

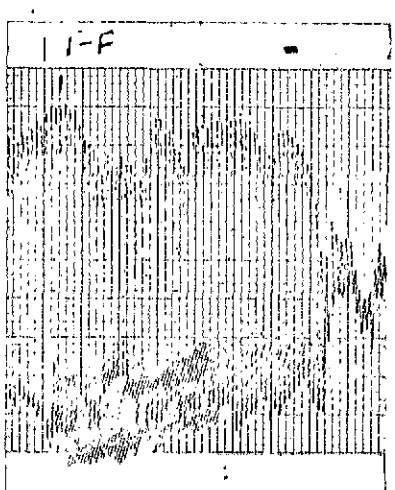

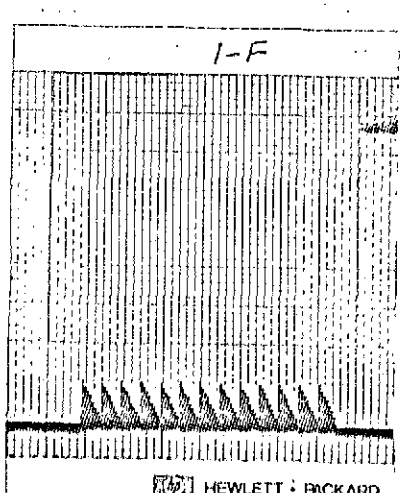

Figure (4.3)

in (1F) depicts a rapid decay more in agreement with the decay in the first part of the time history. Linear response systems produce exponential decays which can be related to system damping ratios. The Auto-Correlator output also applies to nonlinear response systems, and this instrument may present a method of studying them.

The first time history segment (1-B) in Figure (4.4) for Data Point 214 shows a very rapid drop in the peak values followed by a large number of peak values of constant amplitude. The corresponding autocorrelation function exhibits approximately constant amplitude peaks. Segment (1-C) shows peaks that decay for a greater number of cycles but that once again flatten out. The cycles in the autocorrelation function (1-C) corresponding to the zero and first seven time lags tau supports the time history by showing a more rapid envelope decay. The time history for Segment (1-D) depicts a consistent decay for 32 cycles and the corresponding autocorrelation function (1-D) supports this observation with a rapid envelope decay.

Figure (4.5) shows an expended time scale for the autocorrelator outputs already shown in Figure (4.4) for Data Point 214. The departure of the seven stairstep functions away from the ideal exponential decay associated with a linear system would serve as an excellent instrument for studying nonlinearities in the flow process. This is the first time that such an instrument has been designed and constructed.

BAGANOFF ASSOCIATES, INC. Report No.: 610

AUTOCORRELATOR DAMPOMETER EVALUATION Date: January 18, 1974

Dwell Data Point 214 Q = 120 PSF
ϕ = 120° Damping Ratio = 1.17%

Input: Time History of Base x Strain Gage

Output: Autocorrelation Function Repeated

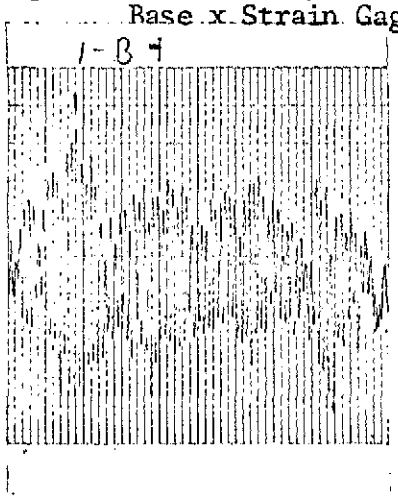

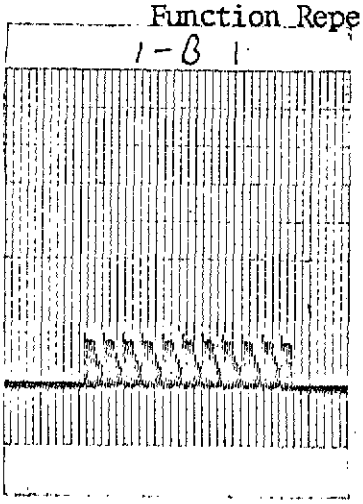

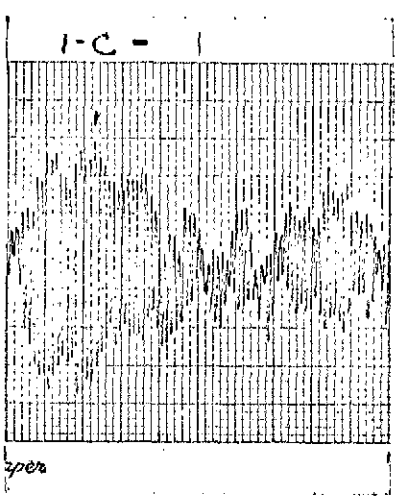

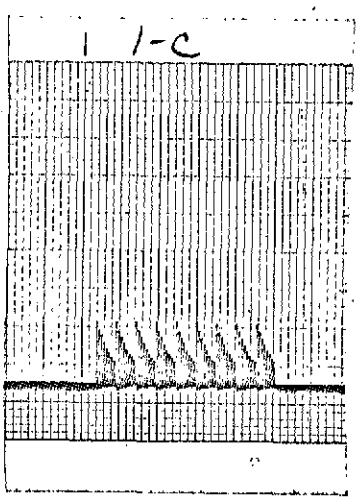

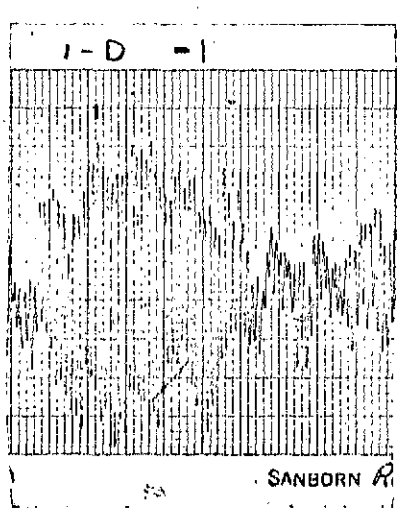

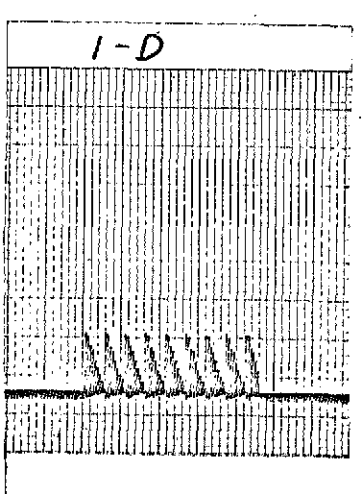

Figure (4.4)

BAGANOFF ASSOCIATES, INC. Report No.: 610

AUTOCORRELATOR DAMPOMETER OUTPUT Date: January 18, 1974

Dwell Data Point 214 Q = 120 PSF
ϕ = 120° Damping Ratio = 1.17%

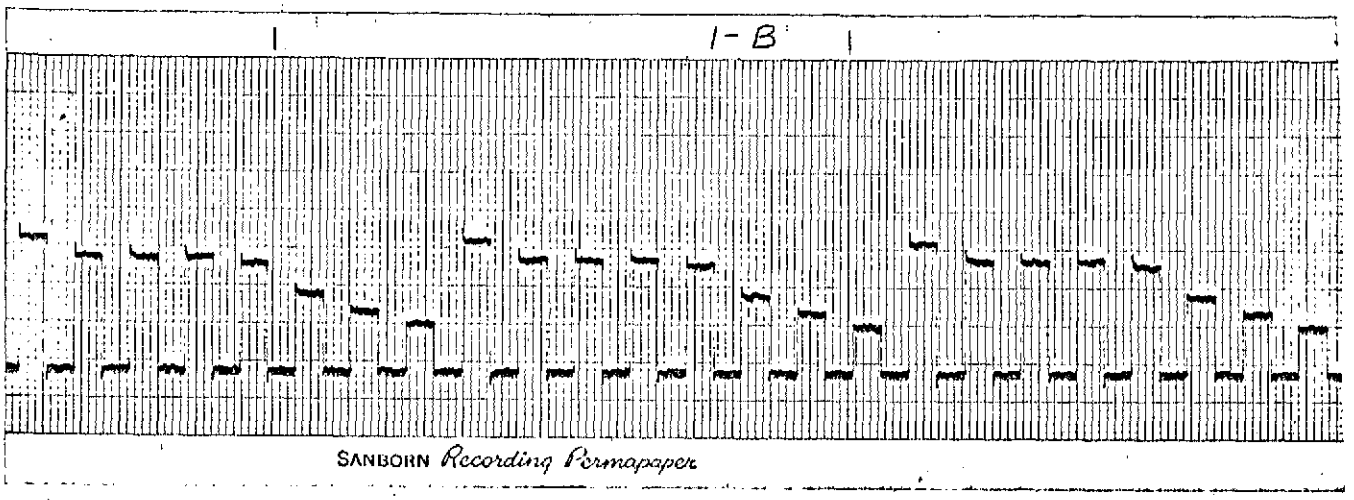

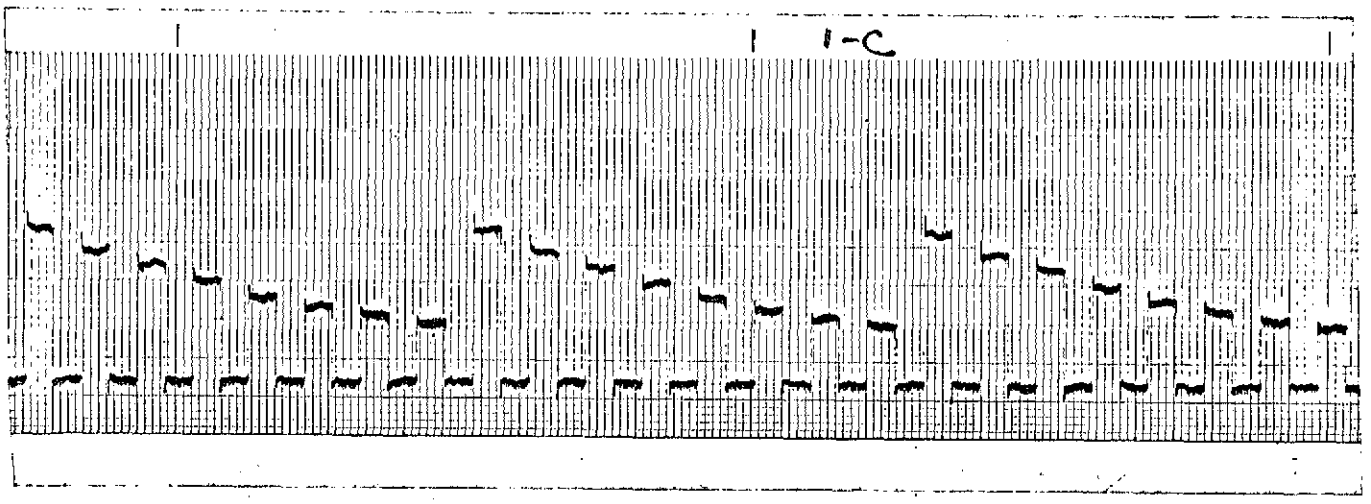

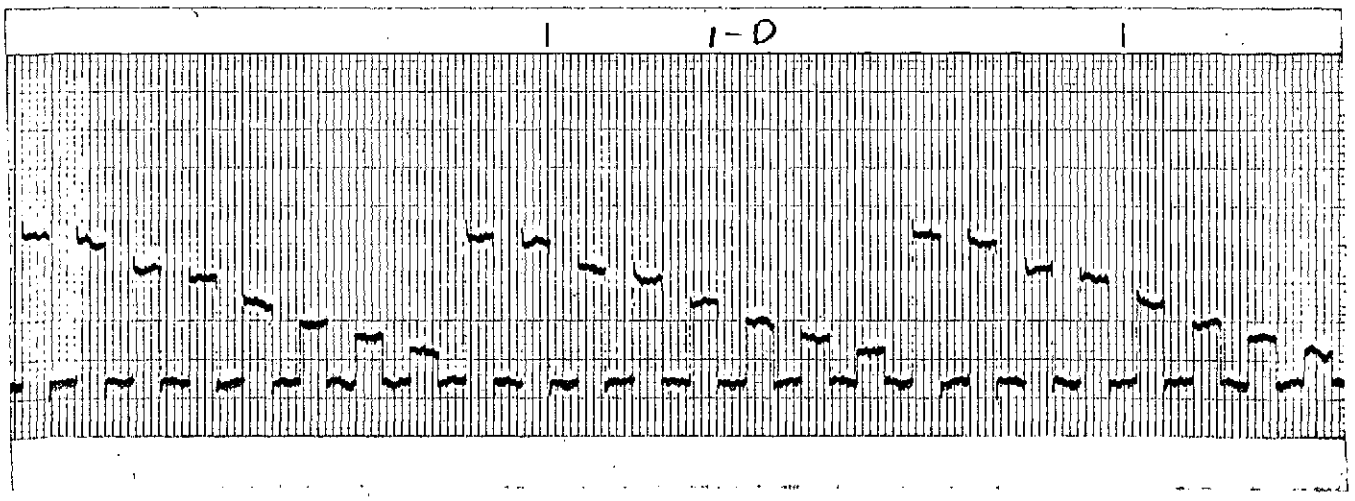

Figure (4.5)

The trigger threshold can be set so that in a normal five minutes wind tunnel run, whether a sweep or dwell condition, approximately 75 autocorrelation functions would be calculated. A boxcar or exponential decay averager type could be constructed to ensemble average the variable autocorrelator functions for a time period consistent with the stationarity of the flow process. The construction of an autocorrelation averager remains to be recommended as future work. The ensenbled autocorrelation function would then produce a hard number for the system damping ratio in real-time for monitoring on an oscilloscope.

The envelope decay or log-decrement of the ensembled autocorrelation function should produce an unbiased estimate of the true system damping ratio. This is based on the intuitive reasoning that the turbulent boundary layer which imparts a random force to the model at times constructively aids the vehicle motion, and at other times destructively interferes with this motion. There should be no preference for either constructive or destructive interference by the aerodynamic forces involved.

The Autocorrelator Dampometer output can be directly applied to the Log-Ratio Dampometer input as previously discussed for sinusoidal step function applications occurring in the wind tunnel and laboratory. In this case the latter instrument averages the log-ratio between successive

steps of the autocorrelation output. The method of interconnecting these two instruments is shown in Figure (5.1). The Operating Instructions are contained in Figure (5.2). The Computer Simulation Study of the Autocorrelator Dampometer presented in Section (4.2) indicates the power of utilitizing this instrument also for multi-modal analysis applications under sinusoidal step inputs.

Further progress in the development of these techniques requires expertise on the part of the Unsteady Aerodynamics Laboratory at MSFC and computer expertise as exists at BAI.

5.0 DRAWING LISTING

Figure No.	Description	Drawing No.
5.1	Wiring Diagram For Autocorrelator Dampometer Followed By Log-Ratio Dampometer	
5.2	Autocorrelator Operating Instructions	
5.3	Block Diagram Correlator Damping Analyzer	10001A
5.4		10001
5.5		10002
5.6		10003
5.7		10004
5.8		10005
5.9		10006
5.10		10007
5.11		10008
5.12		10009
5.13		10010
5.14		10011
5.15		10012
5.16		10013
5.17		10014
5.18		10015
5.19		10016
5.20		10017
5.21		10018
5.22		10019
5.23		10020
5.24		10021

WIRING DIAGRAM FOR AUTOCORRELATOR

DAMPOMETER FOLLOWED BY LOG-RATIO

DAMPOMETER

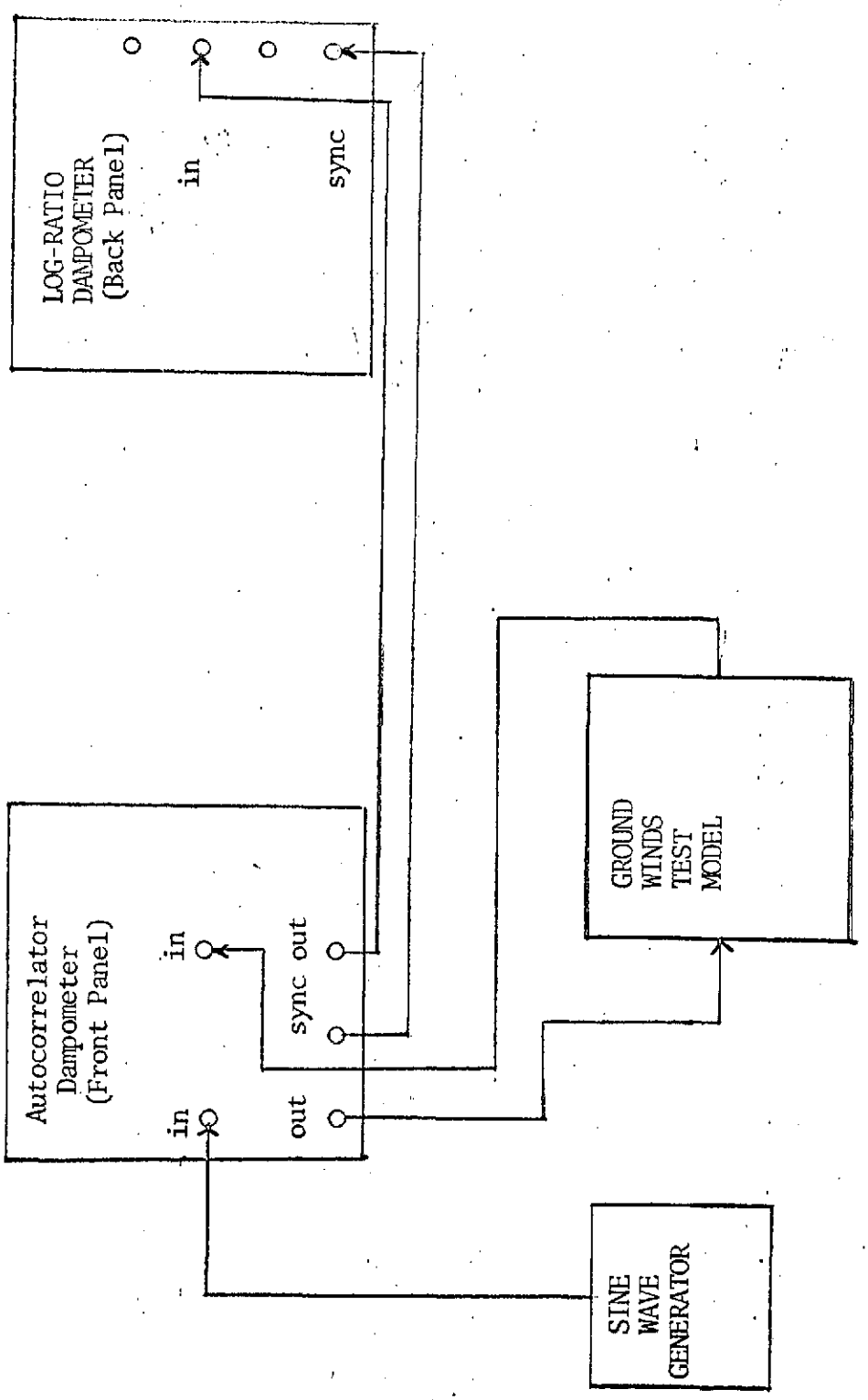

Figure (5.1)

Report No.: 610

AUTOCORRELATOR OPERATING INSTRUCTIONS

Date: January 18, 1974

1. Connect cables as shown in figure 1.

2. Remove top of Dampometer and do the following:
   A. Remove card 1 and replace it with card 12.
   B. Put switch on card 2 in A position.
   C. Put switch on card 9 in A position.
   D. Replace top of cabinet.

3. Turn power on; both units.

SET-UP

4. Set the front panel controls as follows:

   Correlator
   A. OPERATE-CAL switch in CAL.
   B. Depress RESET button.
   C. NEGATIVE PEAK off.
   D. Adjust input level to 1000.

   Dampometer
   A. LIMIT switch to 8.
   B. Depress RESET button.
   C. Adjust level adjust control for a reading of 1.500 on the Dampometer meter.

5. Put Correlator OPERATE-CAL switch in OPERATE position.

6. Set up for a solution is now ready. Set the START and RESET buttons in the following order only:
   A. Correlator RESET
   B. Dampometer RESET
   C. Dampometer START
   D. Correlator RESET

7. For high % damping where only a few cycles are available (above 4%) put the NEGATIVE PEAKS switch in the ON position.

8. Adjust Correlator meter level to about 1000.

9. Proceed as outlined from step 6.

NOTES:

1. A blank meter or a negative answer indicates signal level too high to Dampometer.
2. The CAL position of the OPERATE-CAL switch will put out a 5V signal on the Correlator output.
3. The resolution when using negative peaks is 1/2 true solution.

Figure (5.2)

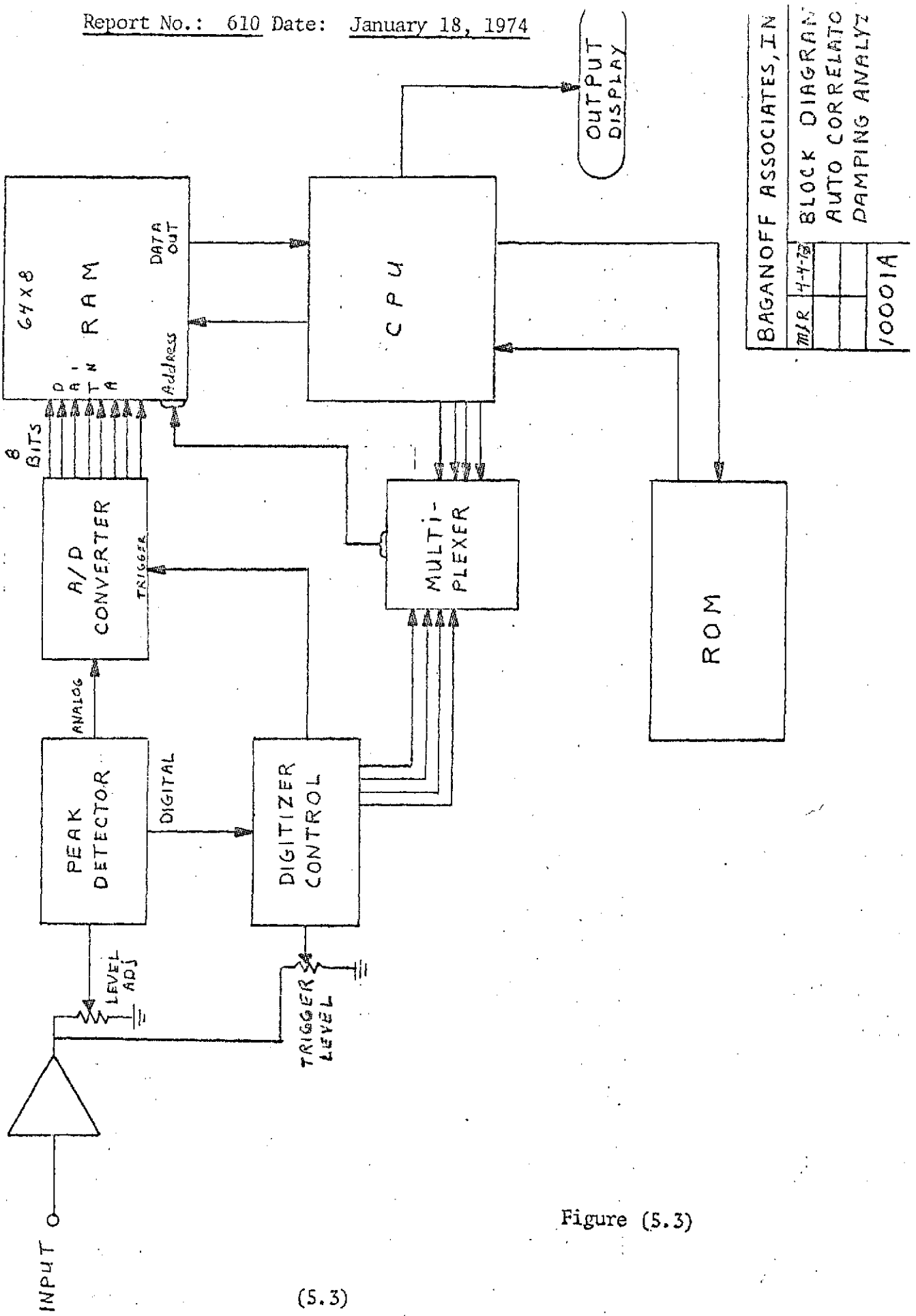
OUTPUT DISPLAY
64X8 RAM
DATA OUT
ADDRESS
DATA IN
8 BITS
CPU
A/D CONVERTER
TRIGGER
MULTI-PLEXER
ROM
ANALOG
PEAK DETECTOR
DIGITAL
DIGITIZER CONTROL
LEVEL ADJ
TRIGGER LEVEL
INPUT
BAGANOFF ASSOCIATES, IN
BLOCK DIAGRAM
AUTO CORRELATO
DAMPING ANALYZ
MLR 4-4-74
100018

Figure (5.3)

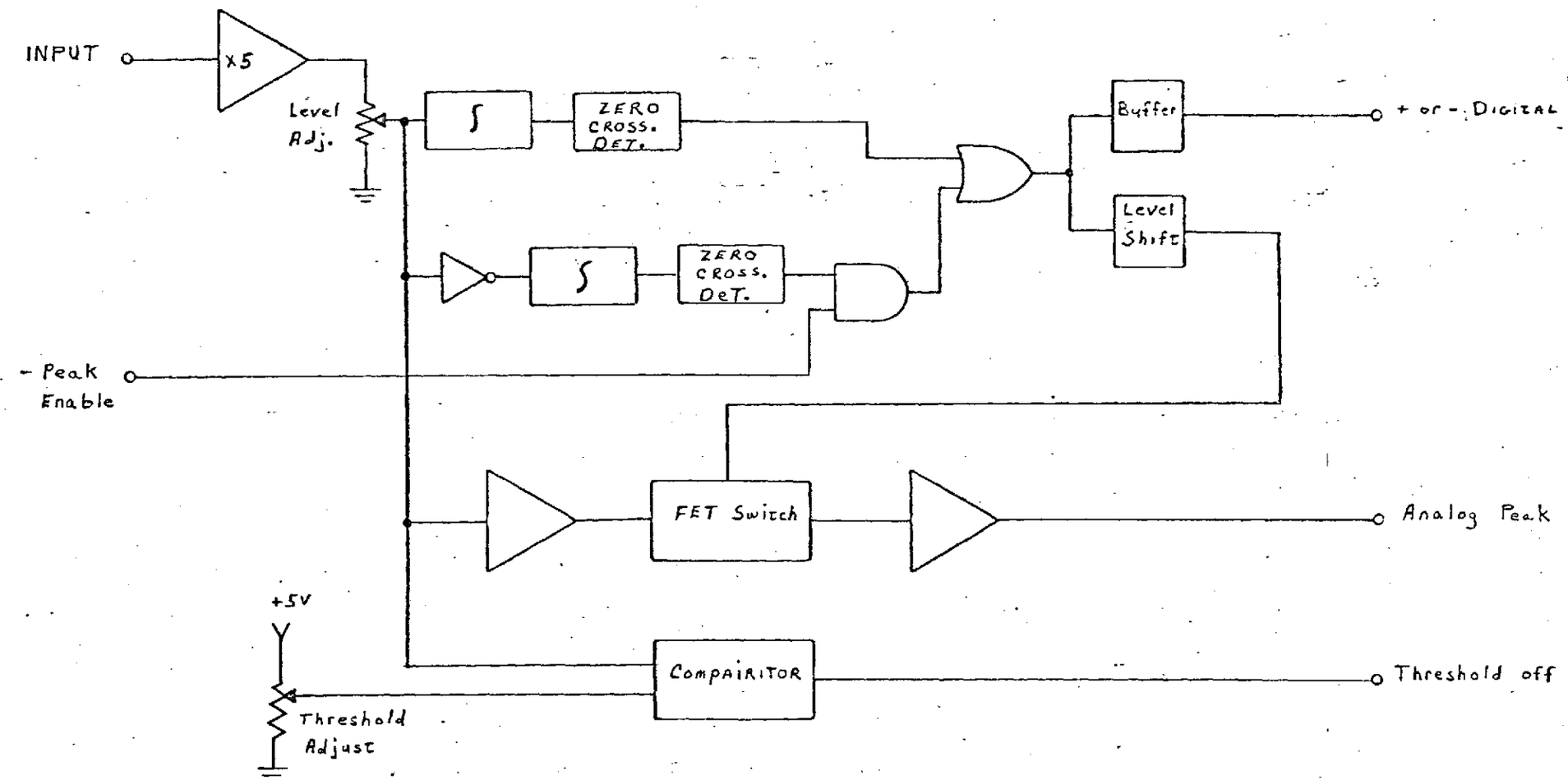

Figure (5.4)

(5.4)

Report No.: 610

Date: January 18, 1974

FOLDOUT FRAME 1

FOLDOUT FRAME 2

BAGANOFF ASSOC. INC.	
2-14R M/R	BLOCK DIAGRAM PEAK DETECTOR
10001	

Notes:
1. MC845P Vcc = pin 14
GND = pin 7

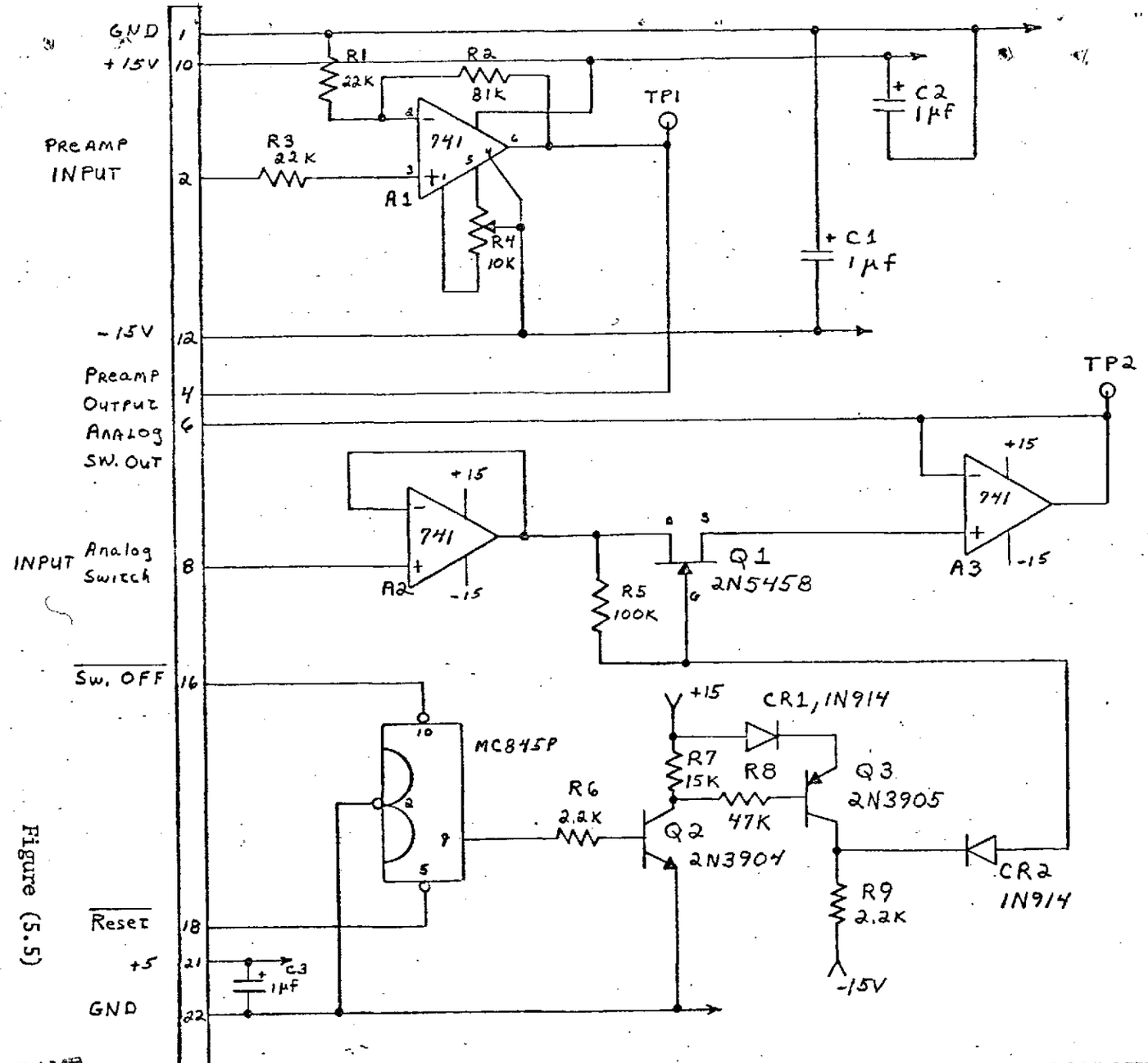

Figure (5.5)

(5.5)

Report No.: 610

Date: January 18, 1974

BAGANOFF ASSOC. INC.

2-14-72	M/R	PREAMPLIFIER AND ANALOG SWITCH
10002		

FOLDOUT FRAME 1

FOLDOUT FRAME 2

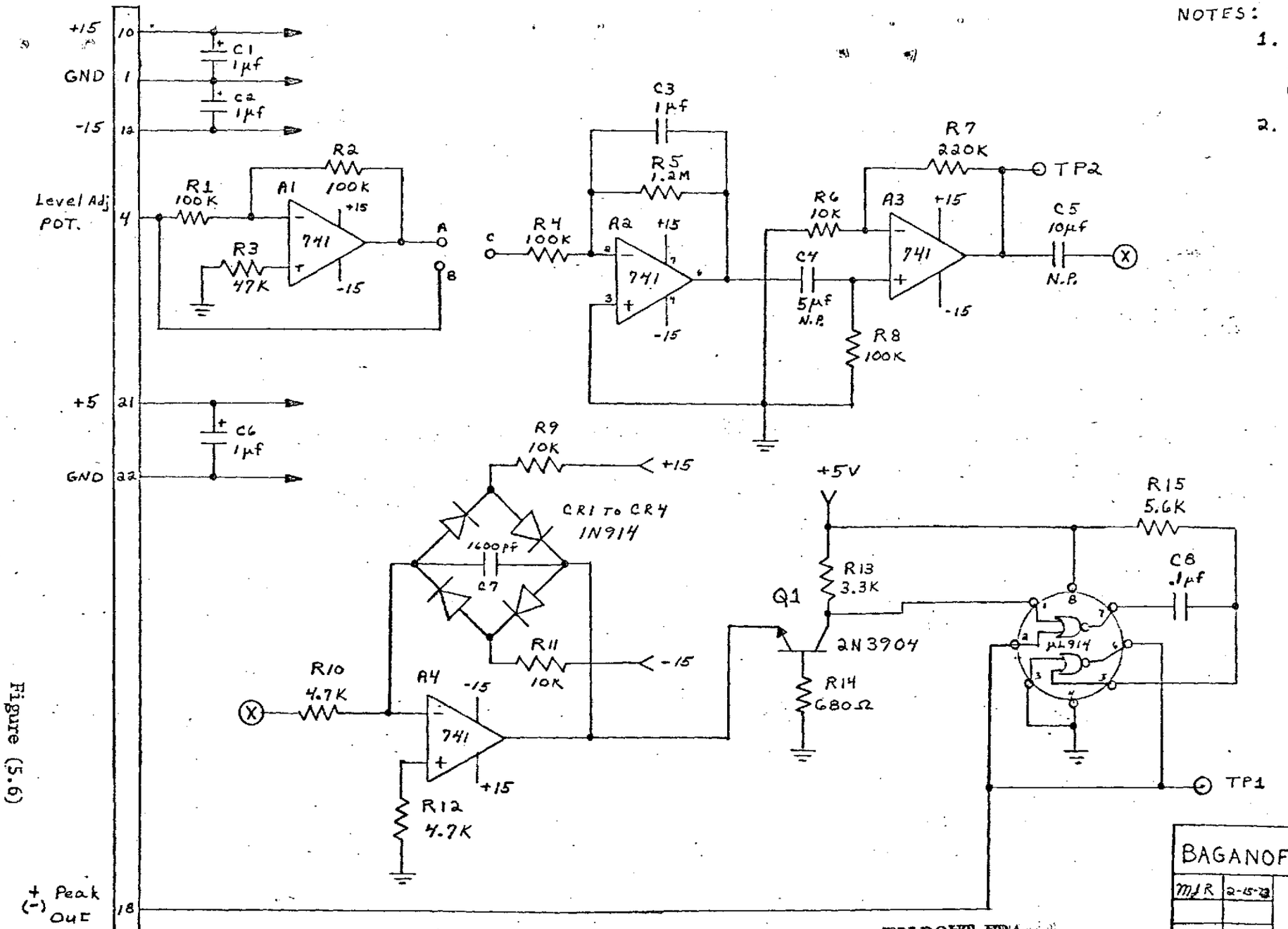

NOTES:

1. For + Peak omit A1, R1, R2, R3 and connect C to B.
2. For - Peak connect C to A.

Figure (5.6)

(5.6)

Report No.: 610

Date: January 18, 1974

BAGANOFF ASSOC. INC.		
MJR	2-15-73	Posative or Negative Peak Detector
10003		

FOLDOUT FRAME

FOLDOUT FRAME

2

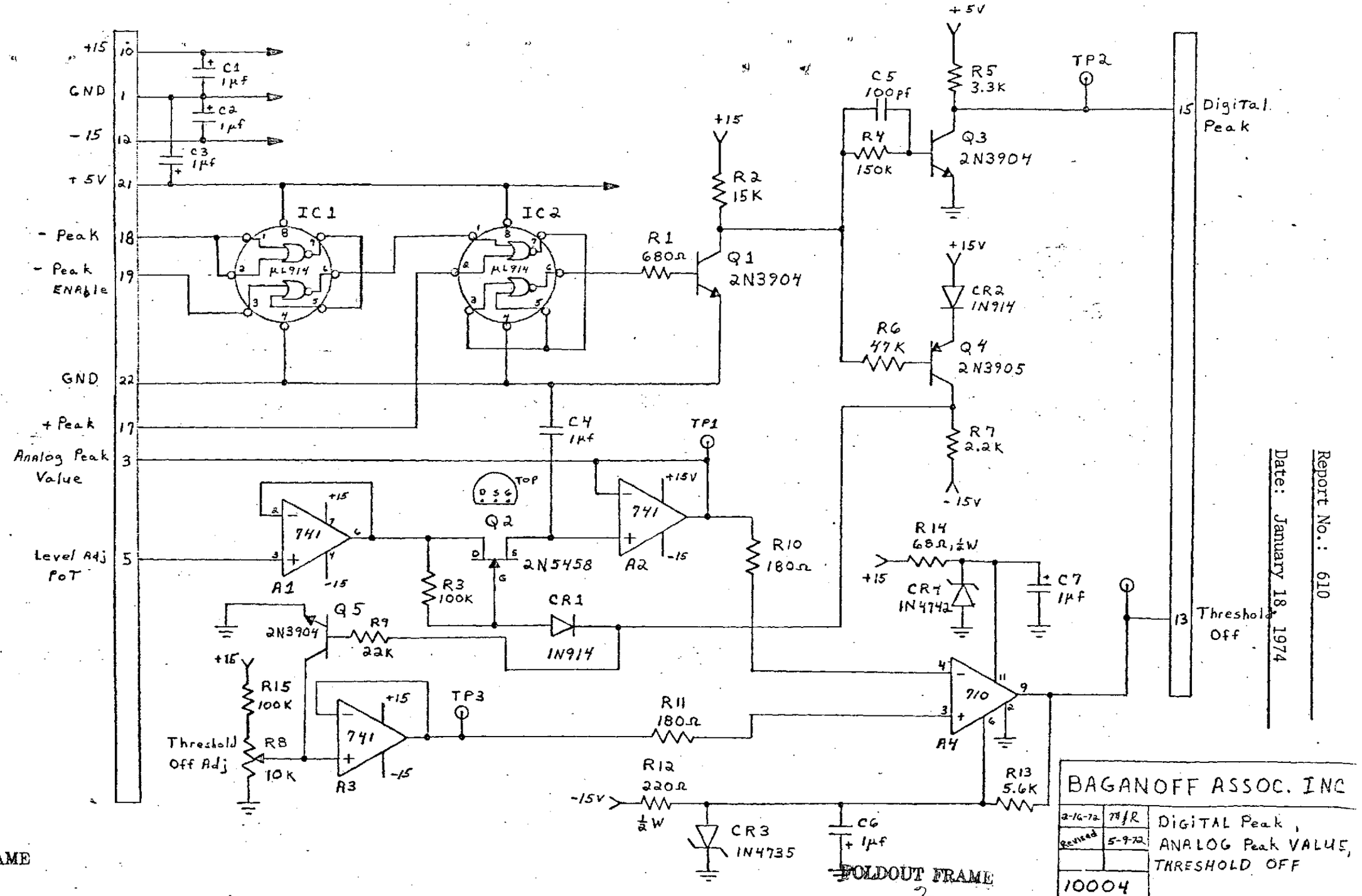

(5.7)

Figure (5.7)

Report No.: 610

Date: January 18, 1974

BAGANOFF ASSOC. INC

2-14-72	TJR	DIGITAL Peak, ANALOG Peak VALUE, THRESHOLD OFF
Revised	5-9-72	
10004		

FOLDOUT FRAME

FOLDOUT FRAME 2

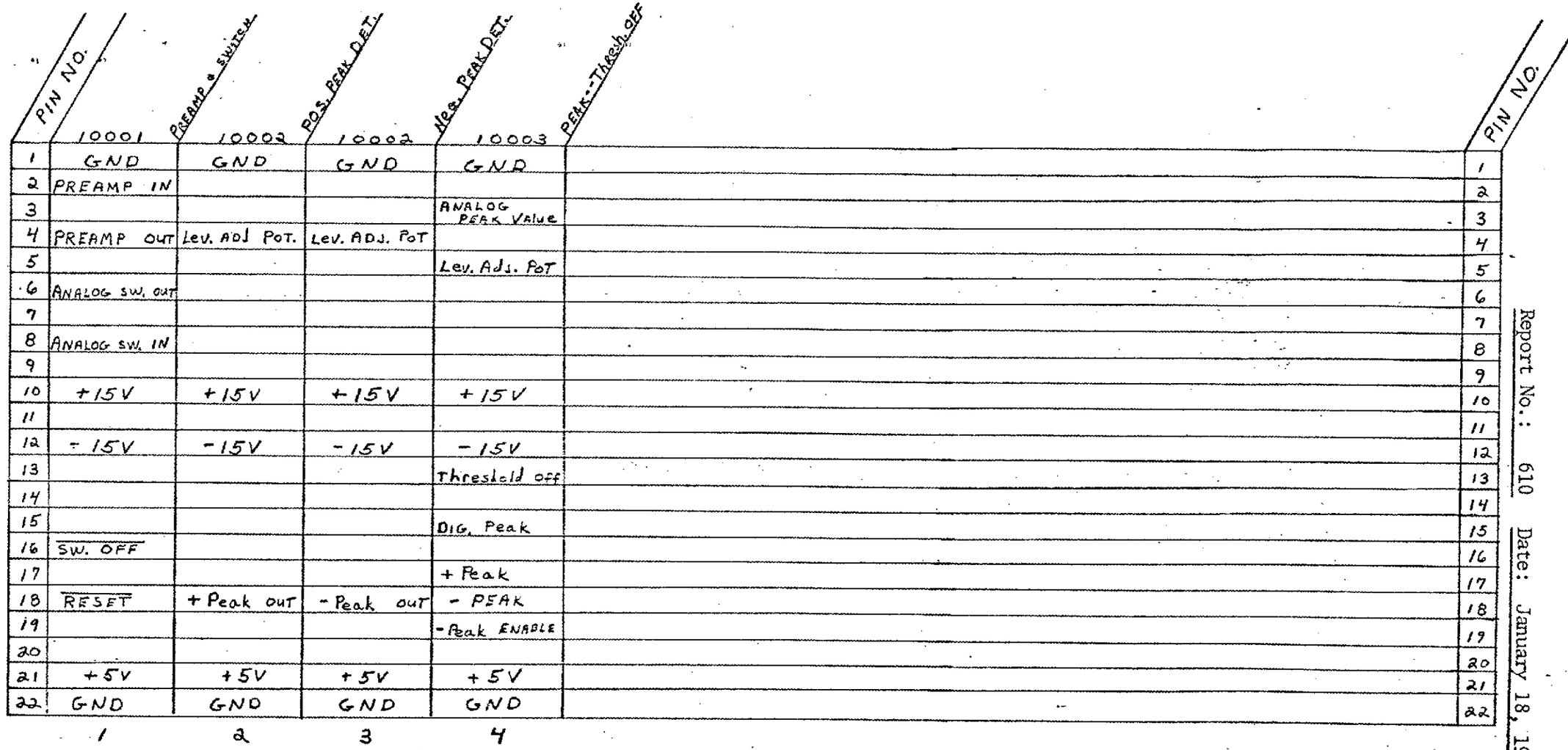

PIN NO.	10001	PREAMP & SWITCH 10002	POS. PEAK DET. 10002	NEG. PEAK DET. 10003	PEAK-THRESH. OFF	PIN NO.
1	GND	GND	GND	GND		1
2	PREAMP IN					2
3				ANALOG PEAK VALUE		3
4	PREAMP OUT	LEV. ADJ POT.	LEV. ADJ. POT			4
5				LEV. ADJ. POT		5
6	ANALOG SW. OUT					6
7						7
8	ANALOG SW. IN					8
9						9
10	+15V	+15V	+15V	+15V		10
11						11
12	-15V	-15V	-15V	-15V		12
13				THRESHOLD OFF		13
14						14
15				DIG. PEAK		15
16	$\overline{\text{SW. OFF}}$					16
17				+ PEAK		17
18	$\overline{\text{RESET}}$	+ PEAK OUT	- PEAK OUT	- PEAK		18
19				- PEAK ENABLE		19
20						20
21	+5V	+5V	+5V	+5V		21
22	GND	GND	GND	GND		22
	1	2	3	4		

(5.8)

Report No.: 610 Date: January 18, 1974

Figure (5.8)

FOLDOUT FRAME 1

FOLDOUT FRAME 2

BAGANOFF ASSOC. INC.

5-24-72	M/R
10005	

P. C. CARD FILE

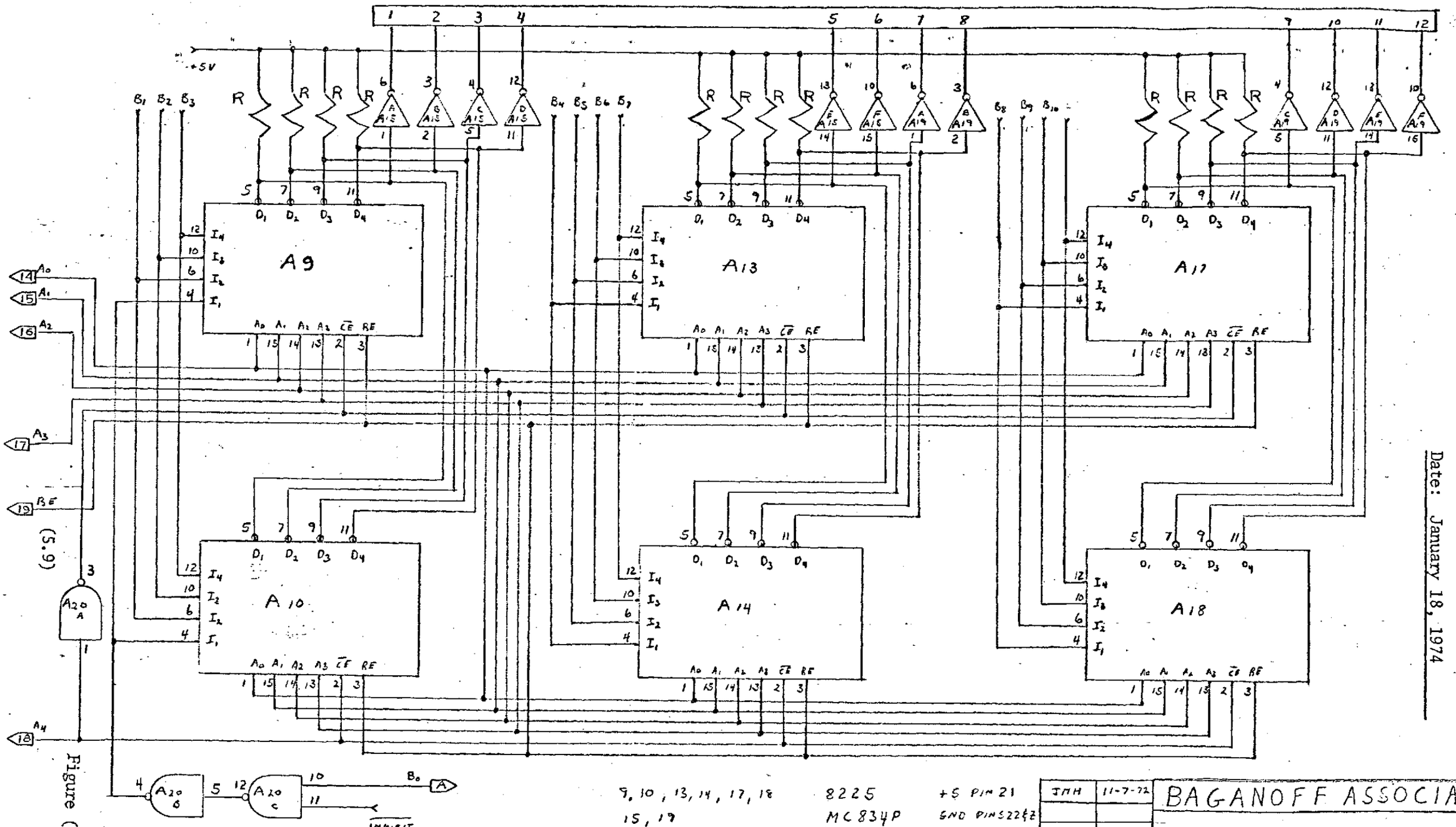

Figure (5.9)

9, 10, 13, 14, 17, 18
15, 19
20

8225
MC834P
MC857P

+5 PIN 21
GND PINS 22 & 2

FOLDOUT FRAME

FOLDOUT FRAME 2

JMH	11-7-72	BAGANOFF ASSOCIATE
		MEMORY
		10006

Report No.: 610

Date: January 18, 1974

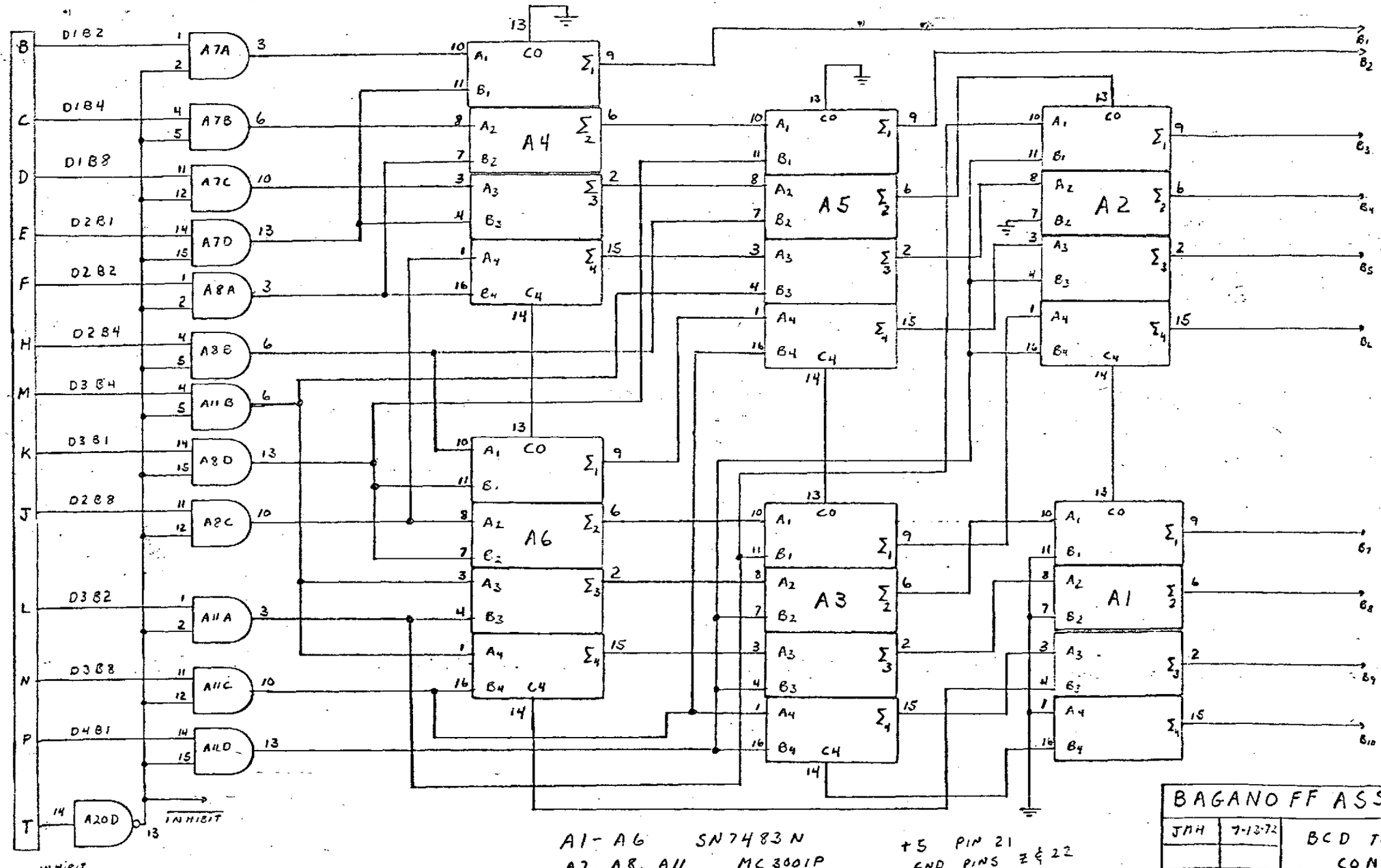

FOLDOUT FRAME 1

FOLDOUT FRAME 2

Figure (5.10)

(5.10)

Report No.: 610

Date: January 18, 1974

BAGANOFF ASSOCIATES

JMH	7-13-72	BCD TO BINARY CONVERTER
10007		

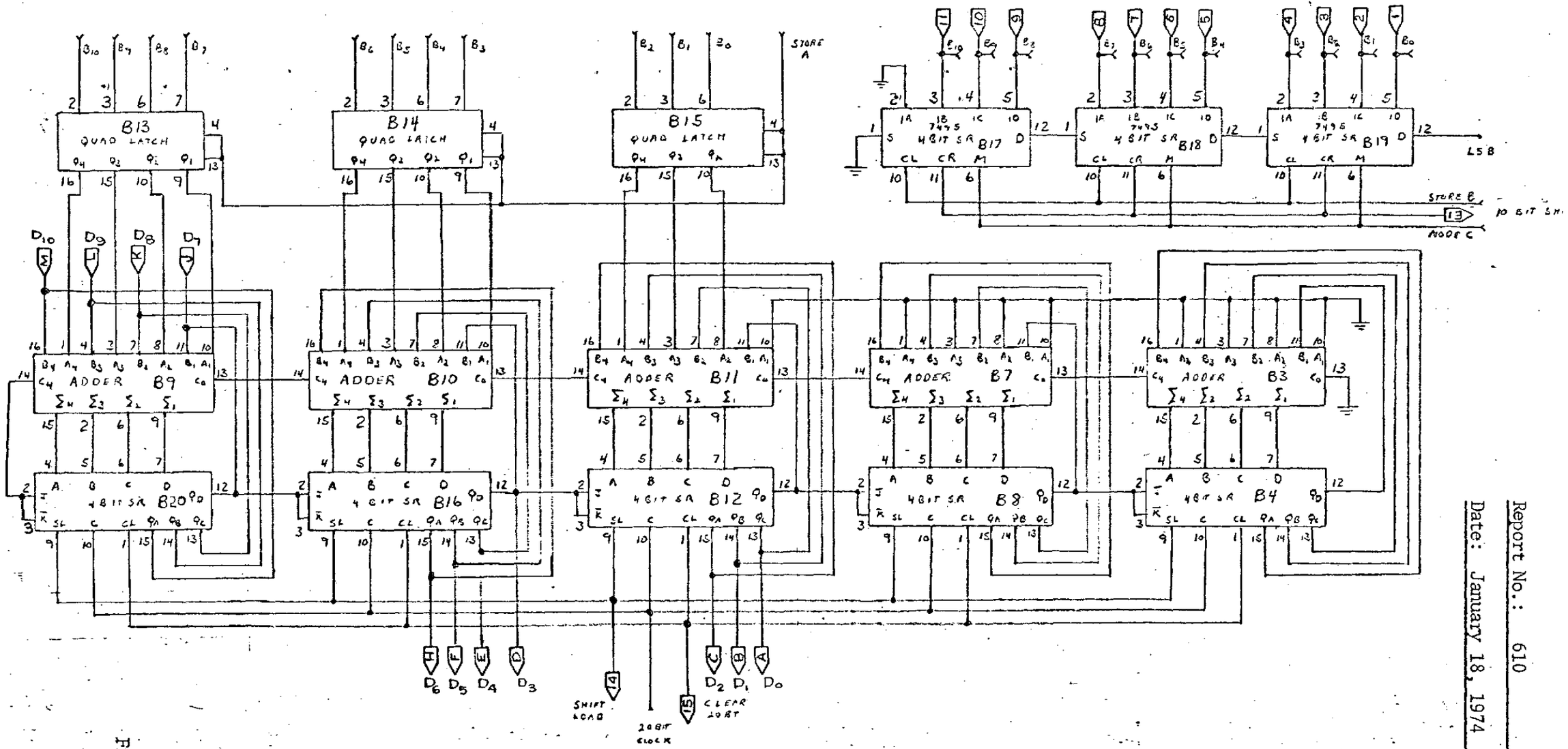

Figure (5.11)

(5.11)

Report No.: 610

Date: January 18, 1974

PART OF CARD "B"

FOLDOUT FRAME

FOLDOUT FRAME

BAGANOFF ASSOCIATES		
JMH	7-14-72	MULTIPLYER
10008		

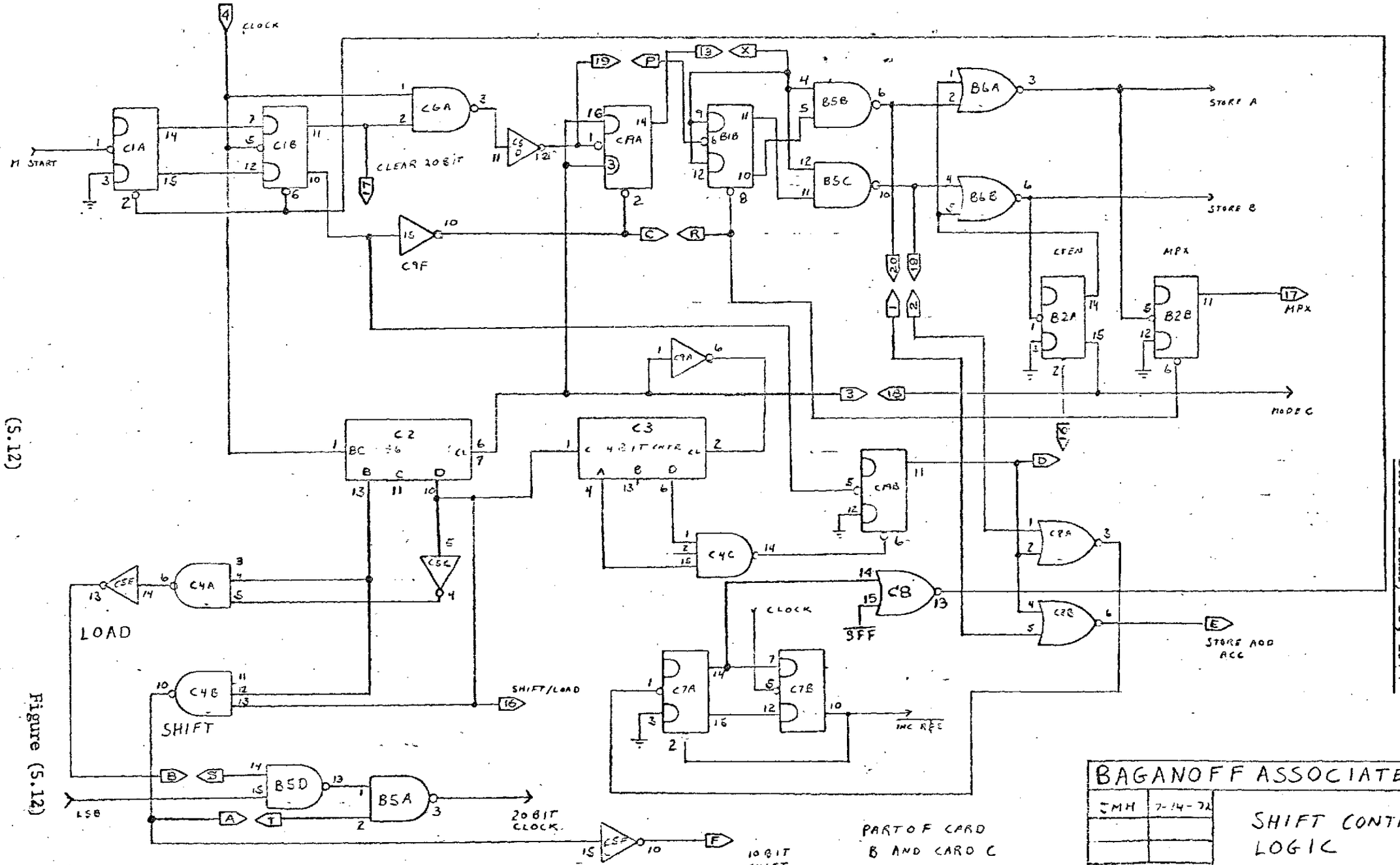

Figure (5.12)

(5.12)

Report No.: 610
Date: January 18, 1974

BAGANOFF ASSOCIATES

EMH	7-14-72

SHIFT CONTROL LOGIC

10009

FOLDOUT FRAME

FOLDOUT FRAME 2

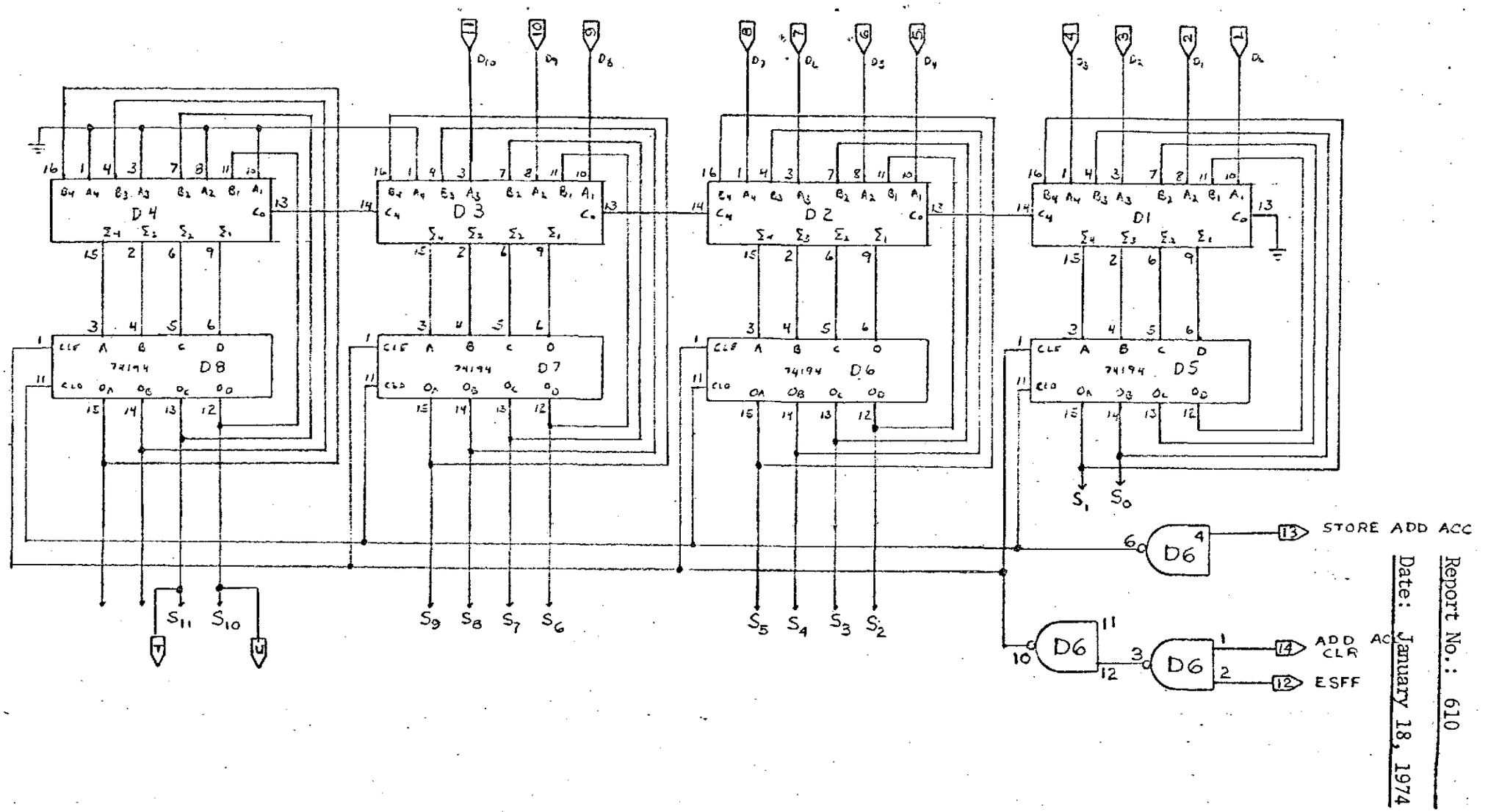

(5.13)

Figure (5.13)

Report No.: 610

Date: January 18, 1974

BAGANOFF ASSOCIATES	
JAH	7-14-72
10010	

SUMMER

FOLDOUT FRAME 1

FOLDOUT FRAME 2

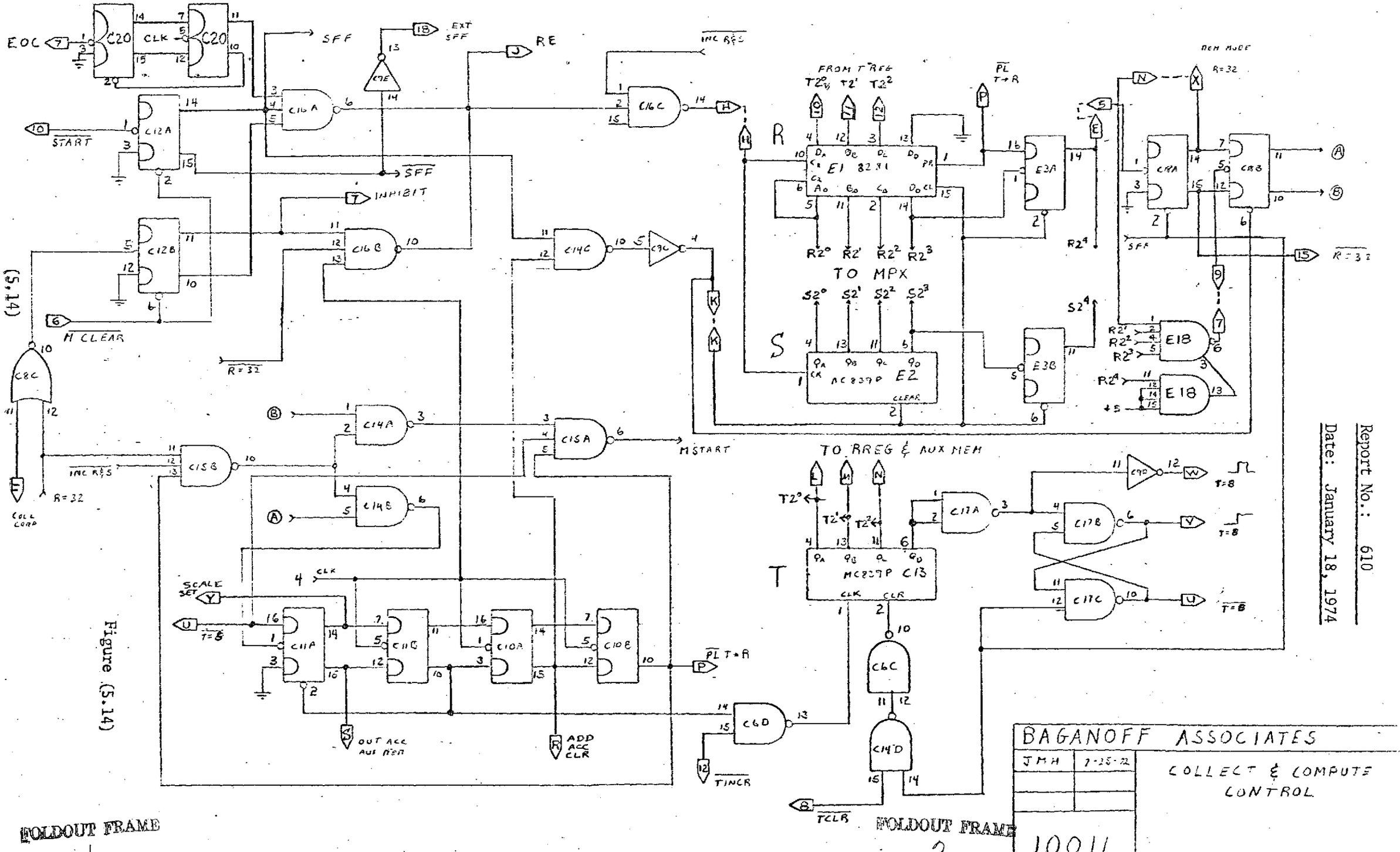
EOC
C20
CLK
SFF
EXT SFF
RE
INC R&S
START
C12A
C16A
C16C
C12B
C16B
C14C
C9C
INHIBIT
M CLEAR
R=32
C8C
C14A
C15A
C15B
C14B
MSTART
CALL COMP
SCALE SET
CLK
C11A
C11B
C10A
C10B
OUT ACC AUX MEM
ADD ACC CLR
PL T→R
C6D
TINCR
FROM T REG
T2^0 T2^1 T2^2
R
E1 82S1
R2^0 R2^1 R2^2 R2^3
TO MPX
S
S2^0 S2^1 S2^2 S2^3
S2^4
AC839P E2
CLEAR
E3A
E3B
NEW MODE
R=32
C9A
C9B
R2^4
SFF
R=32
E1B
E1B
+5
TO RREG & AUX MEM
T
MC839P C13
CLK CLR
T2^0 T2^1 T2^2
C13A
C13B
C13C
C9D
T=8
C6C
C14D
TCLR
FOLDOUT FRAME 1
FOLDOUT FRAME 2
BAGANOFF ASSOCIATES
JMH 7-25-72
COLLECT & COMPUTE CONTROL
10011
Report No.: 610
Date: January 18, 1974

Figure (5.14)

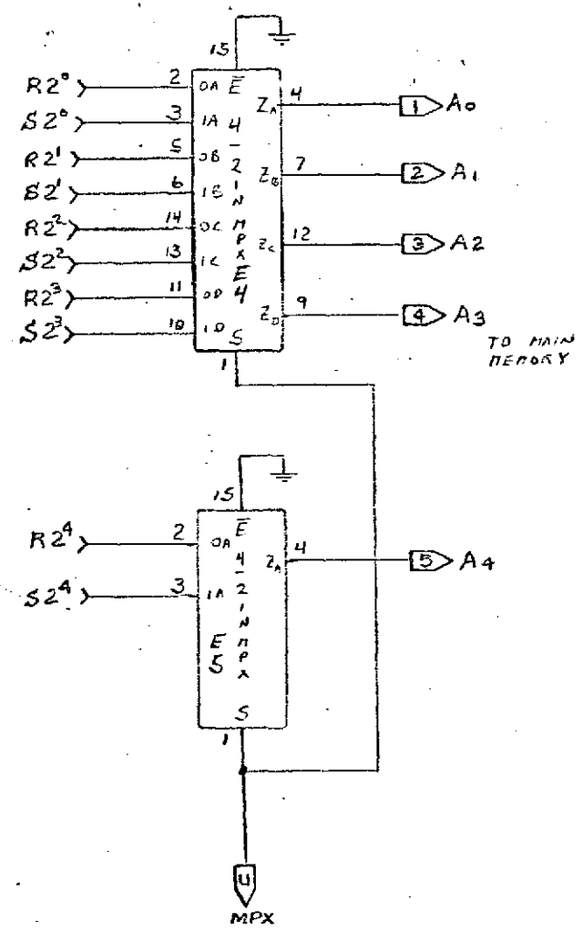

Figure (5.15)

(5.15)

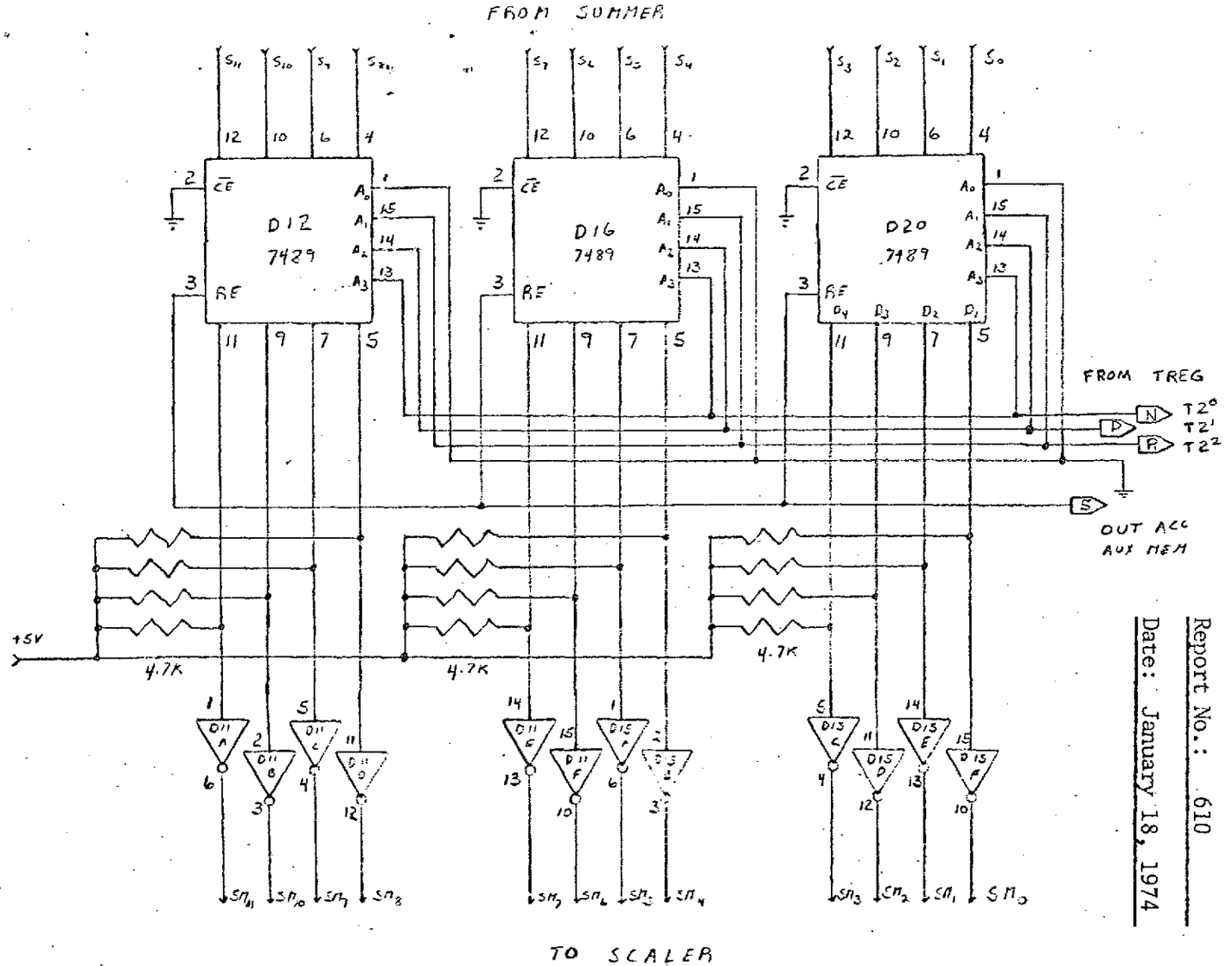

Report No.: 610

Date: January 18, 1974

BAGANOFF ASSOCIATES

JMH	7-25-72
10012	

AUX MEMORY & MAIN MEMORY MULTIPLEXER

FOLDOUT FRAME

FOLDOUT FRAME 2

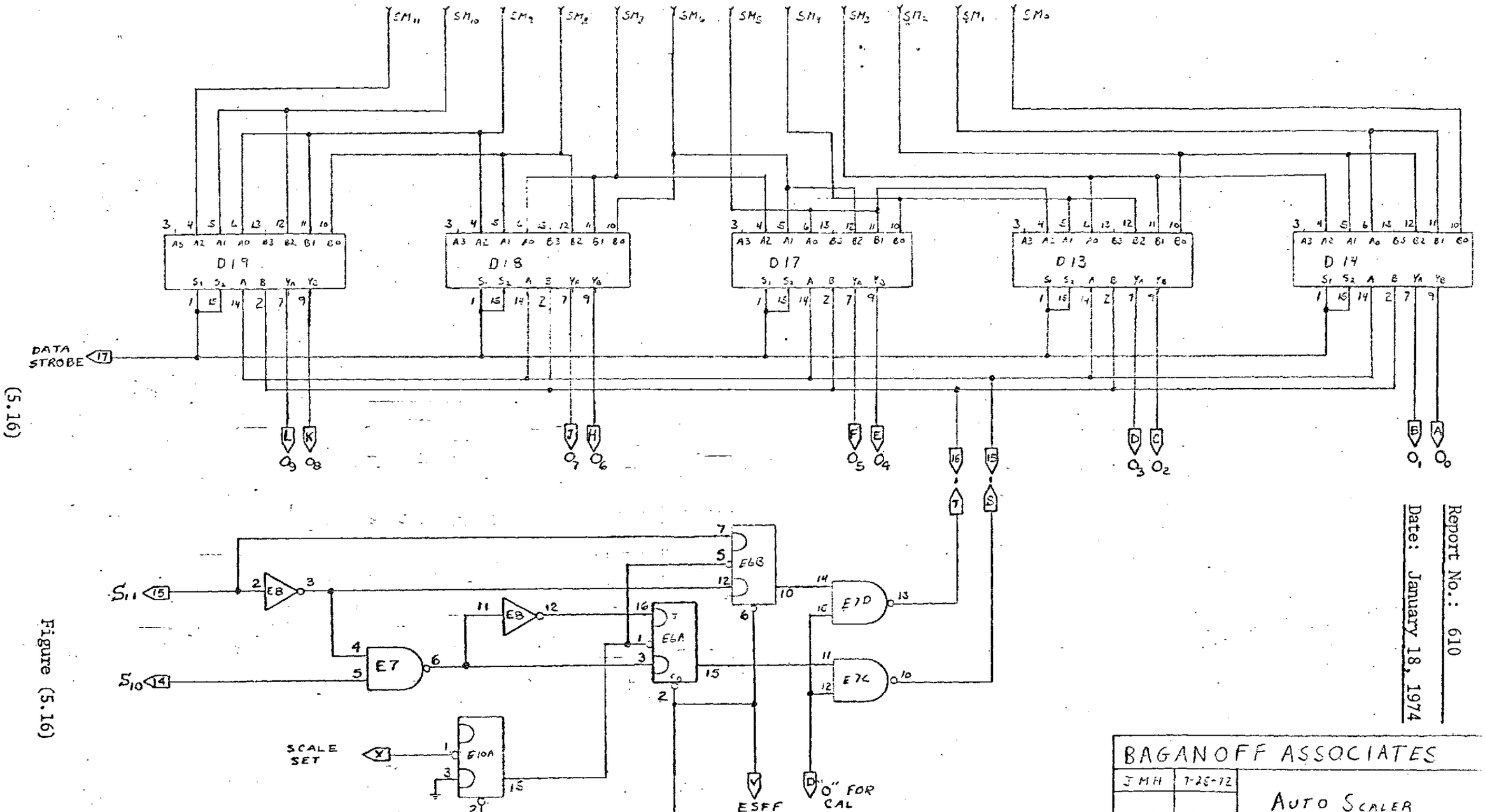

Figure (5.16)

(5.16)

Report No.: 610

Date: January 18, 1974

BAGANOFF ASSOCIATES	
J M H	7-25-72
10013	

AUTO SCALER

FOLDOUT FRAME

FOLDOUT FRAME

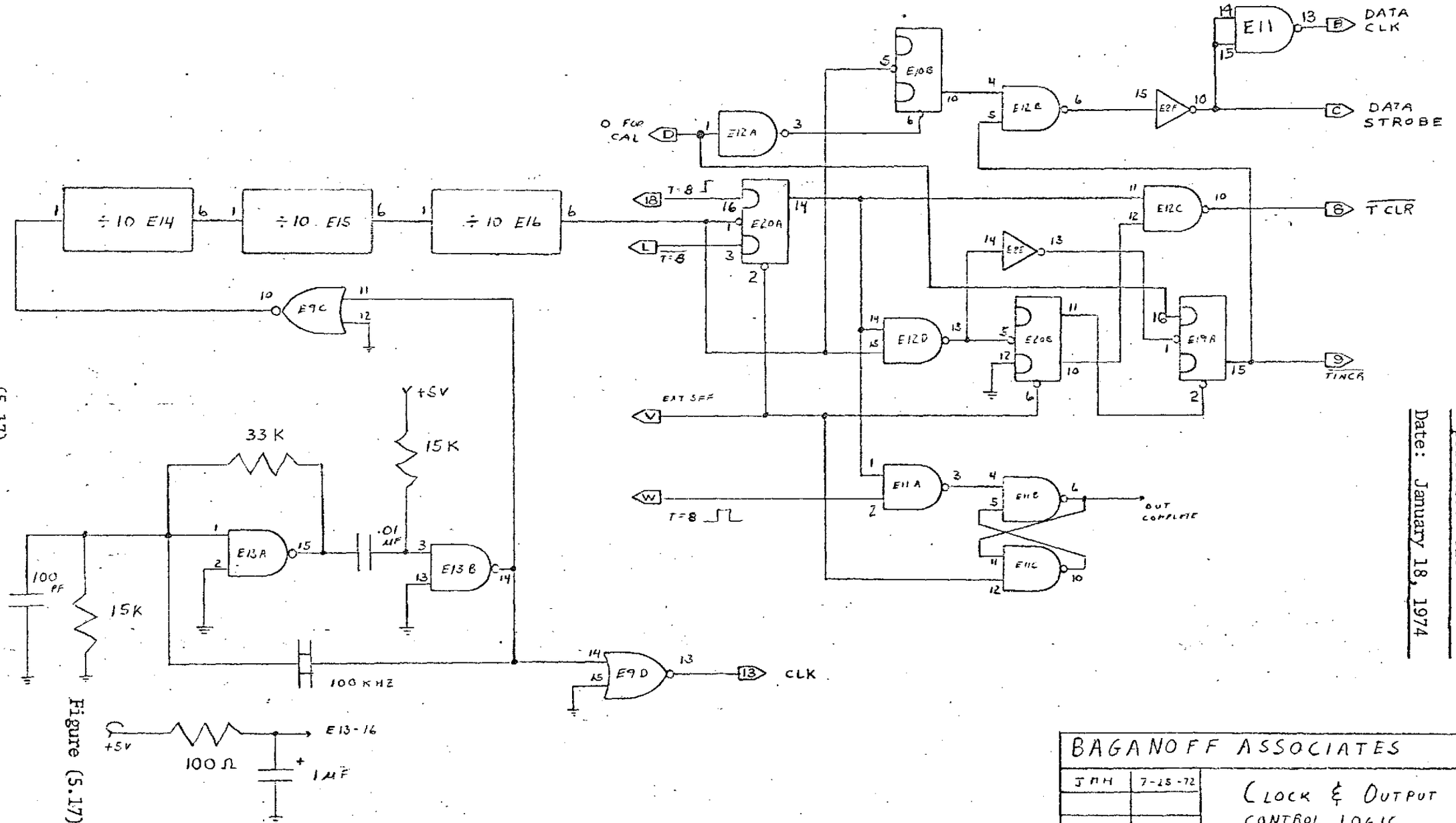

(5.17)

Figure (5.17)

Report No.: 610

Date: January 18, 1974

BAGANOFF ASSOCIATES	
JMH	7-25-72
10014	

CLOCK & OUTPUT CONTROL LOGIC

FOLDOUT FRAME

FOLDOUT FRAME 2

(5.18)

CARD A

4	3	2	1
7483	7483	7483	7483
8	7	6	5
MC3001P	MC3001P	7483	7483
12	11	10	9
	MC3001P	74891 8225	74891 8225
16	15	14	13
	MC834P	74891 8225	74891 8225
20	19	18	17
MC857P	MC834P	74891 8225	74891 8225

Figure (5.18)

CARD B

4	3	2	1
74195	7483	7473	7476
8	7	6	5
74195	7483	MC1810P	MC846P
12	11	10	9
74195	7483	7483	7483
16	15	14	13
74195	7475	7475	7475
20	19	18	17
74195	7495	7495	7495

Report No.: 610

Date: January 18, 1974

BAGANOFF ASSOCIATES

JMH	7-24-72
10015	

CARD LAYOUT

FOLDOUT FRAME 1

FOLDOUT FRAME 2

CARD C

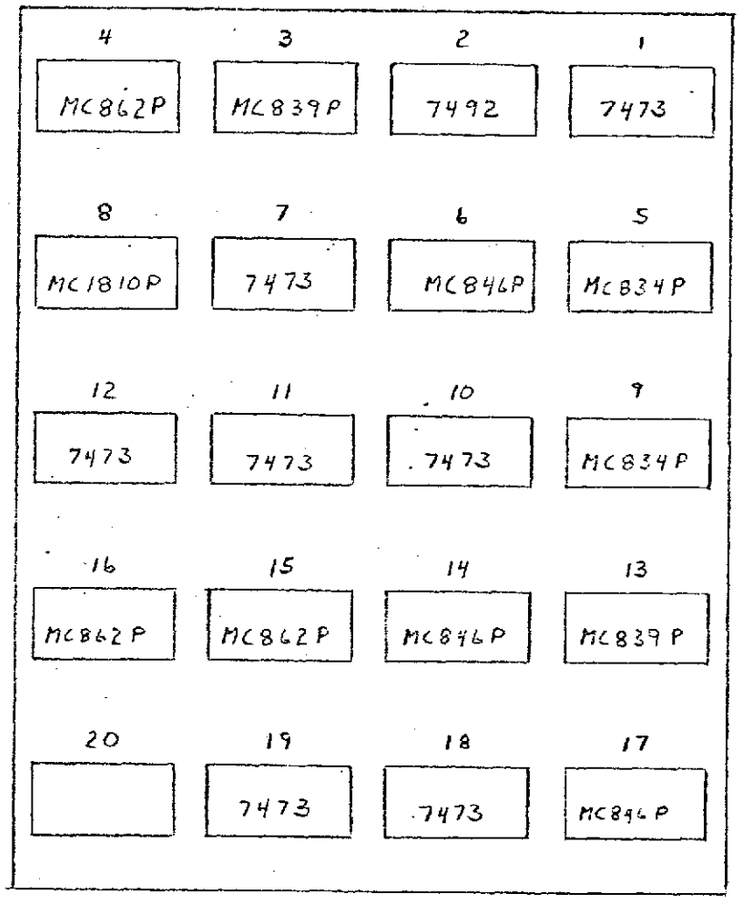

(5.19)

Figure (5.19)

CARD D

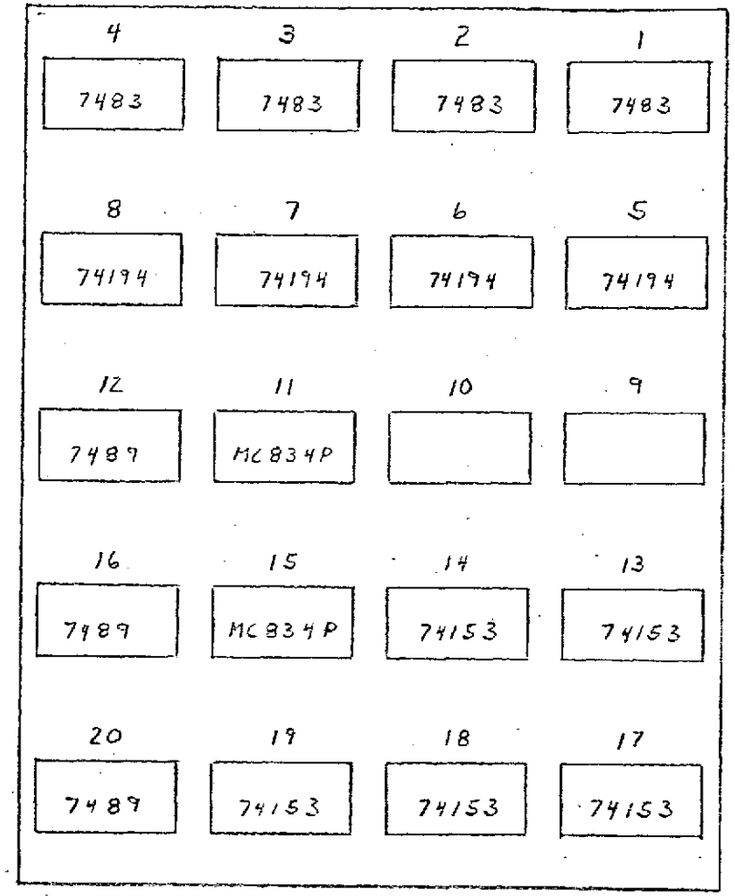

Report No.: 610

Date: January 18, 1974

BAGANOFF ASSOCIATES

JMH	7-25-72

CARD LAYOUT

10016

FOLDOUT FRAME 1

FOLDOUT FRAME 2

CARD E

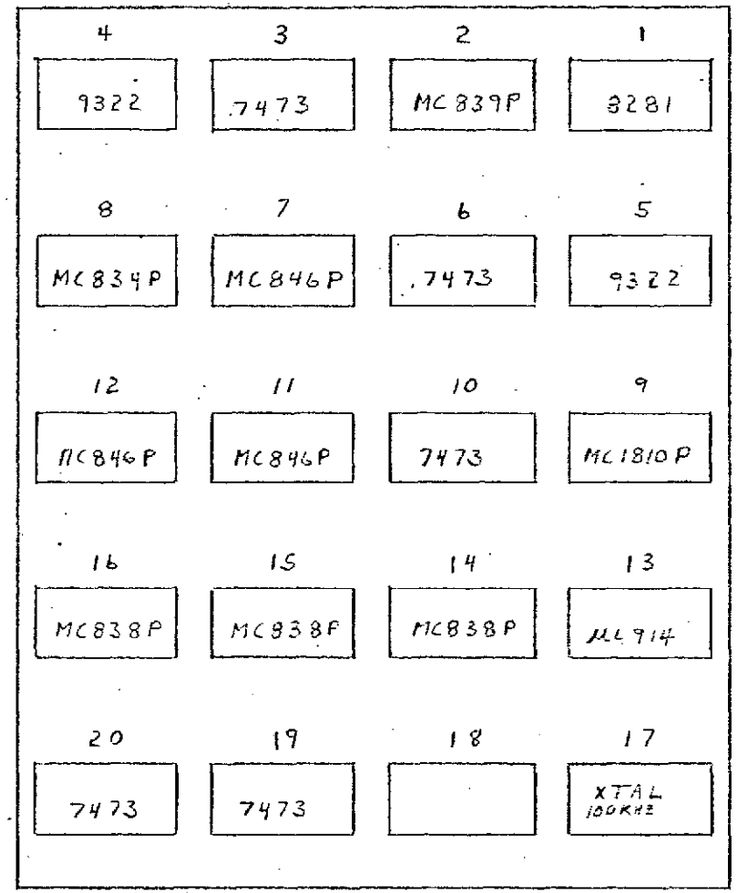

(5.20)

Figure (5.20)

Report No.: 610

Date: January 18, 1974

BAGANOFF ASSOCIATES

JMH	7-25-72

CARD LAYOUT

10017

FOLDOUT FRAME 1

FOLDOUT FRAME 2

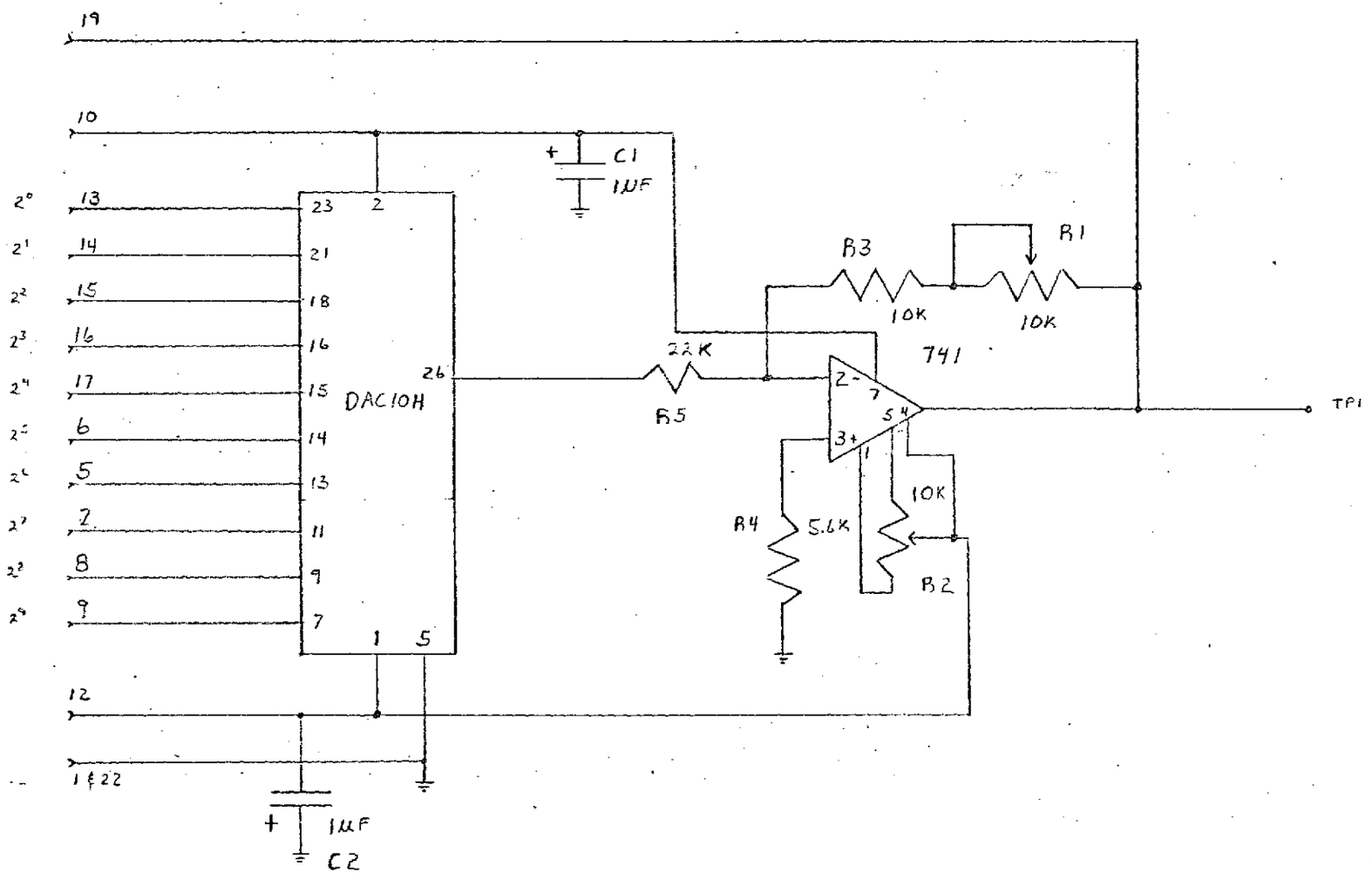

Figure (5.21)

(5.21)

Report No.: 610

Date: January 18, 1974

FOLDOUT FRAME 1

FOLDOUT FRAME 2

BAGANOFF ASSOCIATES

JMH	8-17-72
10018	

DIGITAL TO ANALOG CONVERTER

	E					D				C				B				A			
1	GND		A	1	A14	F13	A	1	BA	BT	A	1	B20	D1	A	1	A1	P1-A	A	1	B1
2			B	2	A15	F14	B	2	BB	BS	B	2	B19	D2	B	2	A2	P1-B	B	2	B2
3		D17	C	3	A16	F15	C	3	BC	BR	C	3	B18	D3	C	3	A3	P1-C	C	3	B3
4		P1-d	D	4	A17	F16	D	4	BD	B16	D	4	E13	D4	D	4	A4	P1-D	D	4	B4
5	DH	C5	E	5	A18	F17	E	5	BE	D13	E	5	EE	D5	E	5	A5	P1-E	E	5	B5
6	DF		F	6	P1-e	F6	F	6	BF	B13	F	6	10001-18 P1-f	D6	F	6	A6	P1-F	F	6	B6
7	DJ	CH	H	7	C9	F5	H	7	BH	EH	H	7	P1-BB	D7	H	7	A7	P1-H	H	7	B7
8	DK		J	8	C8	F7	J	8	BJ	A19	J	8	E8	D8	J	8	A8	P1-J	J	8	B8
9	DL	CK	K	9	C12	F8	K	9	BK	EK	K	9		D9	K	9	A9	P1-K	K	9	B9
10	+16V	CU	L	10	CL/DN	F9	L	10	BL	E10/DN	L	10	P1-h	D10	L	10	A10	P1-L	L	10	B10
11			M	11	CM/DP		M	11	BM	E11/DP	M	11	10003-13	D11	M	11	A11	P1-M	M	11	B11
12	-15V	C15	N	12	CN/DR	CL/E10	N	12	EV/C18	E12/DR	N	12	E9		N	12		P1-N	N	12	
13	DA	CP	P	13	C4	CM/E11	P	13	CE	EP	P	13	BX	C19	P	13	CF	P1-P	P	13	
14	DB		R	14	DU	CN/E12	R	14	CR	D14	R	14		CC	F	14	C16		R	14	E1
15	DC	D15	S	15	DT	CS	S	15	ES	DS	S	15	EN	CB	S	15	C17		S	15	E2
16	DD	D16	T	16		E15	T	16	ET	AT	T	16	B14	CA	T	16	CD	CT	T	16	E3
17	DE	B17	U	17		E14	U	17	EC	EL	U	17	B15		U	17	EU		U	17	E4
18		D12	V	18	CV		V	18		E18	V	18	D12		V	18	C3		V	18	E5
19	P1-a	CW	W	19			W	19		EW	W	19	BP		W	19	C2		W	19	CJ
20		CY	X	20			X	20		EN	X	20		C13	X	20	C1		X	20	
21			Y	21	+5V		Y	21	+5V	EX	Y	21	+5V		Y	21	+5V		Y	21	+5V
22	GND	GND	Z	22	GND	GND	Z	22	GND	GND	Z	22	GND	GND	Z	22	GND	GND	Z	22	GND

(5.22)

Figure (5.22)

Report No.: 610

Date: January 18, 1974

BAGANOFF ASSOCIATES

JMH

BACK OF RACK
DIGITAL

10019

FOLDOUT FRAME 1

FOLDOUT FRAME 2

BAGANOFF ASSOCIATES
FLOW CHART
AUTOCORRELATOR
LJR 2/13/73
10020

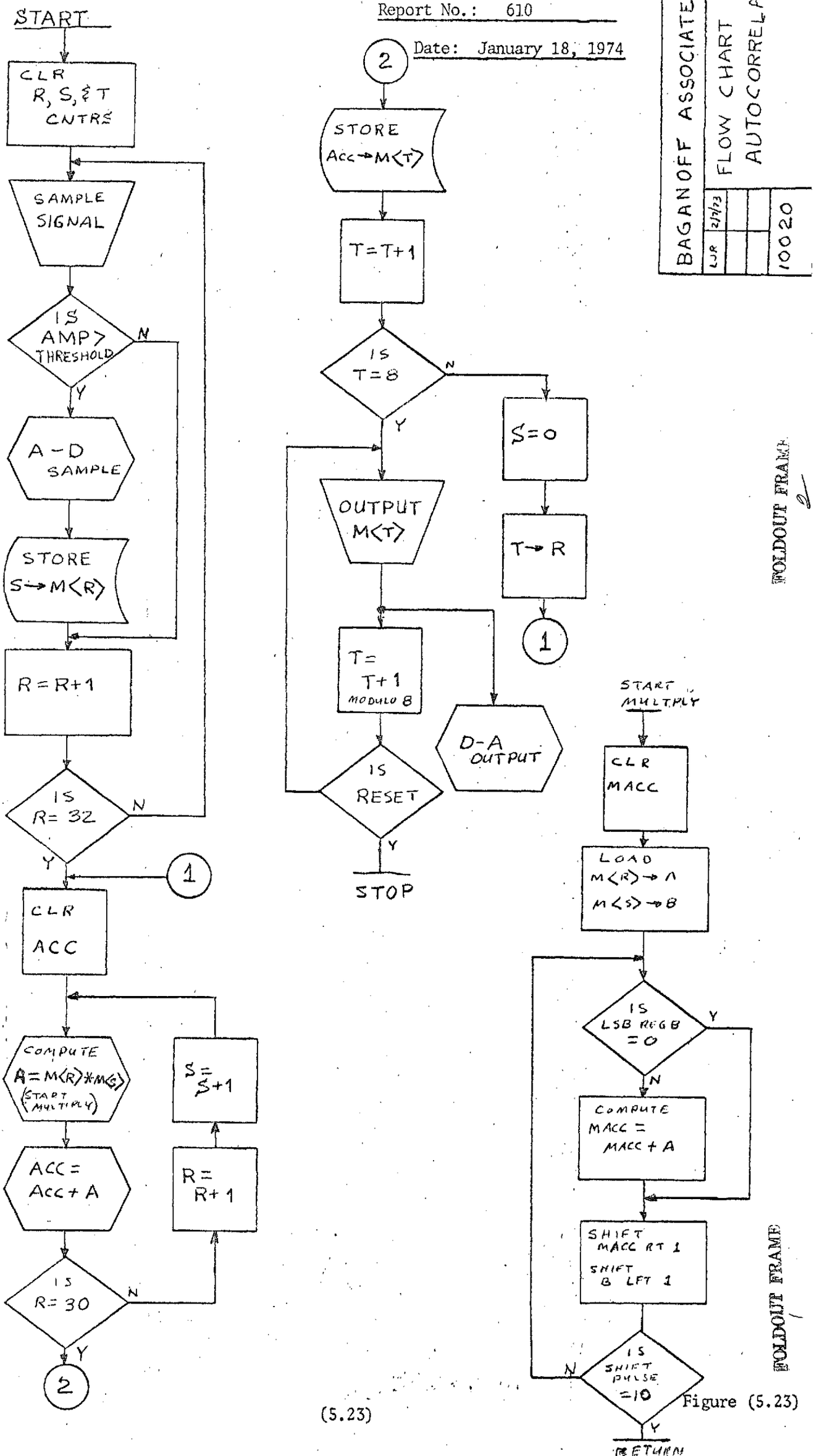

FOLDOUT FRAME 2

FOLDOUT FRAME 1

Figure (5.23)

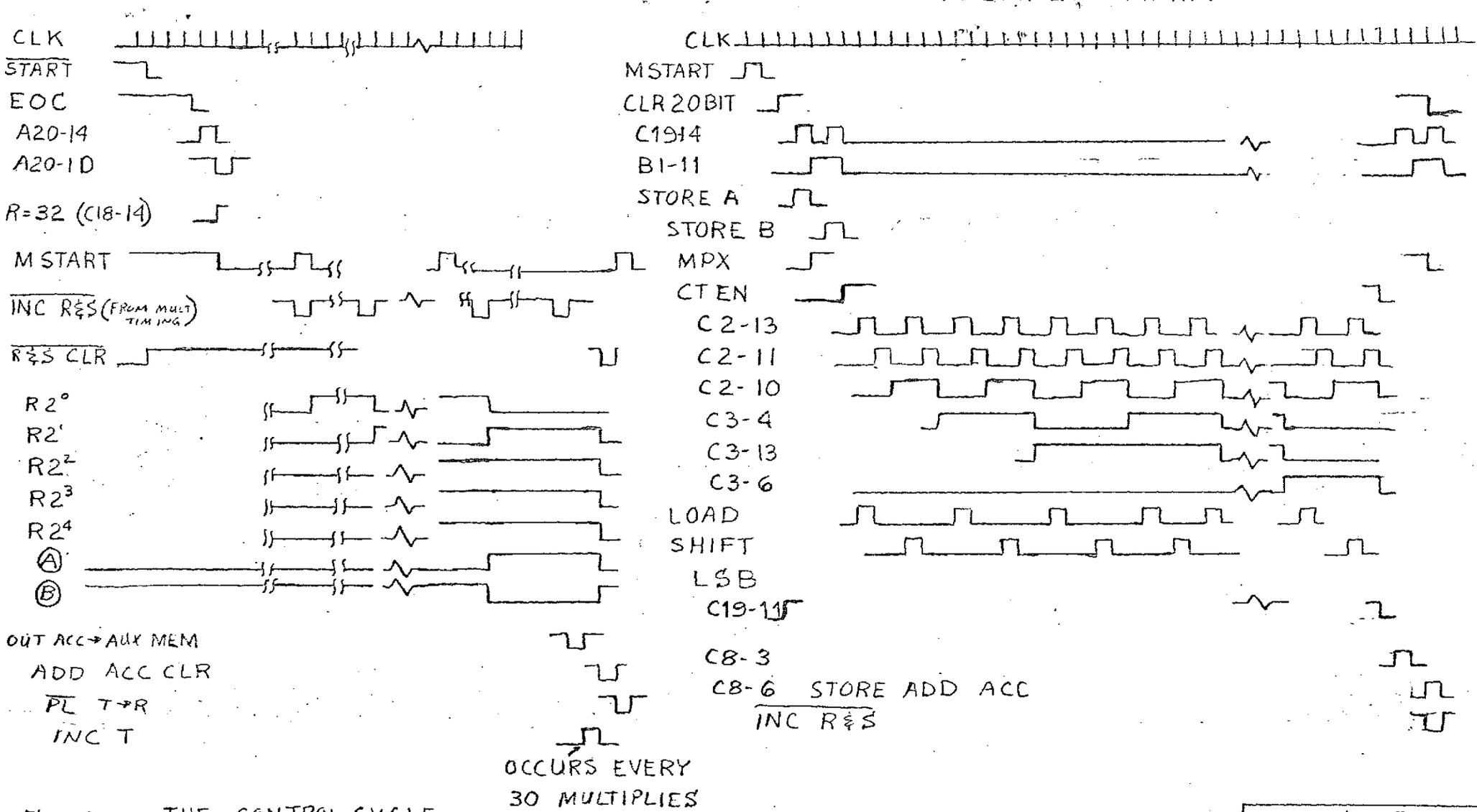

(5.24)

THE CONTROL CYCLE
REPEATS FOR EIGHT CYCLES (T=7)
THEN OUTPUTS THE ANSWERS.

Figure (5.24)

FOLDOUT FRAME

FOLDOUT FRAME 2

Report No.: 610

Date: January 18, 1974

BAGANOFF ASSOCIATES		
LJR	2-13-73	TIMING DIAGRA
10021		